

**Figure 3 | Pathogenic mutants of Parkin are subjected to Ser65 phosphorylation.** (a) Diagram of Parkin protein illustrating the pathogenic mutants used in this study. The Ser65 residue in the Ubl domain is shown as a yellow circle. RING, Ring-finger motif; IBR, in-between-Ring fingers domain. (b) Phos-tag Western blotting for Parkin and Western blotting for PINK1 were performed using Parkin WT and a series of pathogenic mutants as shown in Figure 2a. (c) Endogenous Parkin was also phosphorylated in SH-SY5Y cells after CCCP treatment. Post-nuclear cell lysates from SH-SY5Y cells treated with or without 10  $\mu$ M CCCP for 30 and 60 min were fractionated into mitochondria-rich (Mito) and cytosolic (Cyto) fractions. These two fractions and their combination (Mito + Cyto) were subjected to Phos-tag or normal Western blotting analyses. Endogenous PINK1 was fractionated in the Mito fraction, as previously reported<sup>45</sup>. Lactate dehydrogenase (LDH) and Tom20 were used as cytosolic and mitochondrial marker proteins, respectively. Asterisks: putative cleaved Parkin; dots: non-specific bands.

accumulation of PINK1 (Fig. 4b). The impaired degradation cannot be explained simply by the delayed translocation of Parkin mutants because both mutants completed the mitochondrial translocation by the 6 hr time-point (data not shown and see Fig. 4c). In contrast, the profiles of Parkin expression and autoubiquitination in Parkin S65A- or S65E-expressing cells were comparable with those of WT (Fig. 4b). We also examined whether Ser65 mutations affect the accumulation of proteasome (Fig. 4c) and p62 (Supplementary Fig. S7) at the mitochondria during mitophagy via the immunostaining of the proteasome subunit alpha type 7 ( $\alpha$ 7) and p62. However, there was no evidence that Ser65 mutations inhibit or delay the recruitment of proteasome and p62 to the mitochondria. Finally, we tested whether the Parkin Ubl domain itself is indispensable for the mitochondrial

translocation and the substrate degradation (Supplementary Fig. S8). Interestingly, Parkin mutant lacking the Ubl domain ( $\Delta$ Ubl) showed a mild delay in the mitochondrial translocation, slowed the mitochondrial reorganization to the perinuclear region (Supplementary Fig. S8b and c) and impaired the degradation of mitochondrial outer membrane proteins (Supplementary Fig. S8d). These results suggest that proper regulation of the Parkin Ubl domain through the Ser65 phosphorylation is required not only for efficient translocation to mitochondria as an initial step of mitophagy, but also for the degradation of mitochondrial outer membrane proteins during mitophagy through an as yet unknown mechanism.

## Discussion

A series of *Drosophila* genetic and cell biological studies have clearly demonstrated that PINK1 is required for Parkin-mediated mitochondrial maintenance. The mitophagy of damaged mitochondria is a well-characterised event in which PINK1 and Parkin are involved. However, how PINK1 regulates Parkin is largely unclear. This study has shown that Ser65 in the Ubl domain of endogenous Parkin is phosphorylated in an activated PINK1-dependent manner. In addition to mitochondrial accumulation of PINK1,  $\Delta\Psi$ m depolarisation-dependent PINK1 autophosphorylation has been reported to be an important element for PINK1 activation and Parkin recruitment<sup>19,29</sup>. Consistent with these observations, our investigation of PINK1 siRNA suggests that a lower level of PINK1 is able to phosphorylate Parkin after  $\Delta\Psi$ m depolarisation (Fig. 1c, compare lanes 1 and 4). Our domain analysis of PINK1 demonstrates that intact PINK1 is required for CCCP-dependent Parkin phosphorylation, and the lack of phosphorylation in fibroblasts from a *PARK6* patient implies relevance to the pathogenesis of PD.

The biological significance of this phosphorylation event is suggested by the fact that replacement of Ser65 with alanine or glutamic acid impairs the mitochondrial translocation of Parkin and/or the subsequent mitophagy process. Our observation that maximal phosphorylation of Parkin occurs within 1 hr of CCCP treatment supports the idea that Ser65 phosphorylation is required for the early step of Parkin translocation. In contrast, PINK1 accumulation appears to last at least 6 hr (Fig. 4c and Supplementary Fig. S1b). The difference in time course between PINK1 accumulation and Parkin phosphorylation could be explained by the observation that phosphorylated Parkin is degraded by proteasomal activity. The biochemical evidence that only the phosphorylated form of endogenous Parkin is present in the mitochondrial fraction also implies that Parkin phosphorylation is an essential event for its mitochondrial translocation and subsequent activation (Fig. 3c and Supplementary Fig. S6). Overexpression of PINK1 and Parkin itself leads to mitochondrial translocation of Parkin independently of  $\Delta\Psi$ m depolarization, which suggests that excessive amounts of PINK1 and Parkin do not faithfully reflect endogenous reactions. Our study using *PINK1*<sup>-/-</sup> MEFs stably co-expressing PINK1 and GFP-Parkin might also be saddled with such a problem. We believe that the endogenous observation in which phosphorylated Parkin is accumulated in mitochondria is a more reliable proposal as a molecular model. The delay of exogenous GFP-Parkin S65A in the mitochondrial translocation would indicate that modification of Ser65 is important for Parkin translocation at least. At the same time, another important finding is that pathogenic mutants that lose their translocation activity are also phosphorylated (Fig. 3b), raising the possibility that phosphorylation of Parkin at Ser65 is insufficient for translocation. Thus, Ser65 phosphorylation likely leads to other events in mitochondrial translocation, such as the association or dissociation of protein(s) involved in the mitochondrial translocation of Parkin or the modification of Parkin itself for activation at a different site(s).

Both the S65A and S65E Parkin mutants cannot undergo efficient mitophagy, as indicated by the incomplete degradation of

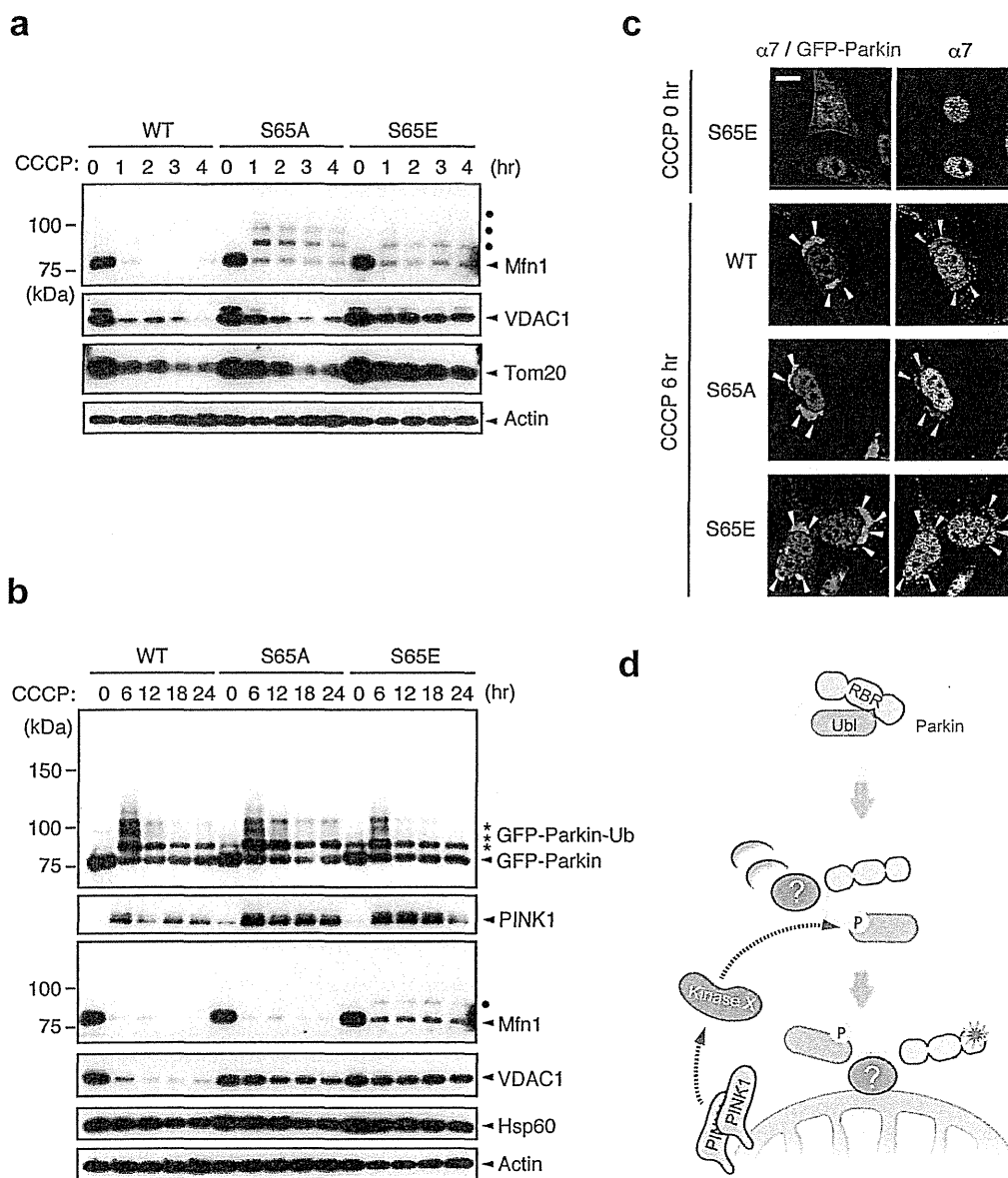


**Figure 4 | Ser65 phosphorylation affects the subsequent autophagy reaction.** (a) CCCP-dependent degradation of mitochondrial outer membrane proteins in PINK1 WT/*PINK1*<sup>-/-</sup> MEFs expressing WT or mutant forms of GFP-Parkin. Mfn1, VDAC1 and Tom20 were used as markers of mitochondrial outer membrane proteins. Actin: a loading control. Dots: ubiquitinated Mfn1. (b) Long-term time-course analysis of CCCP-dependent mitochondrial protein degradation. The degradation of outer membrane proteins was impaired in cells expressing GFP-Parkin S65A or S65E mutations. Hsp60 was used as a marker of mitochondrial matrix proteins. (c) S65A and S65E mutations do not affect proteasome recruitment to the mitochondria during mitophagy. PINK1 WT/*PINK1*<sup>-/-</sup> MEFs expressing WT or mutant forms of GFP-Parkin (green) were treated with 30  $\mu$ M CCCP for 3 or 6 hr. Cells were stained with anti-proteasome subunit alpha type 7 ( $\alpha 7$ , red).  $\alpha 7$ -immunoreactivity was enriched in the nuclei of all three cell genotypes under normal conditions, as displayed in the representative image of S65E (CCCP 0 hr), and overlapped with the aggregated mitochondria (arrowheads) 6 hr after CCCP treatment irrespective of genotype. Similar results were obtained 3 hr after CCCP treatment. Scale bar = 10  $\mu$ m. (d) Model for Parkin translocation and activation. The Parkin Ubl domain masks C-terminal RING-IBR-RING (RBR) domains for E3 activity<sup>46</sup>. A Parkin phosphorylation event at Ser65 (P), combined with unknown factor(s) (?), stimulates the mitochondrial translocation of Parkin, releasing the RBR domains from autoinhibition by the Ubl domain.

the mitochondrial outer membrane proteins. Because inhibition of the degradation of the mitochondrial outer membrane proteins by proteasome inhibitors is reported to block mitophagy<sup>32,35</sup>, it may be that the modification of Parkin Ser65 has a greater than expected impact on the mitophagy process. Although our study does not demonstrate that the S65E mutant behaves exactly like the phosphorylated form of Parkin, the S65E mutant does

translocate to the mitochondria in a similar way to WT, although with slightly impaired efficiency, suggesting that S65E has at least some properties that are similar to phosphorylated Parkin. Currently, it is unknown why S65E also inhibits the later processes of mitophagy. One possible explanation is that rapid degradation of phosphorylated Parkin is required for the proper progression of mitophagy, and S65E may not be degraded effectively. However,

there is no evidence that S65E is more stable than WT, as shown in Figure 4c.

Very recently, Kondapalli *et al.* proposed a model to explain the biological significance of Ser65 phosphorylation, in which Ser65 phosphorylation relieves autoinhibition of Parkin E3 activity by the Ubl domain<sup>18</sup>. This model may explain the depolarised  $\Delta\Psi_m$ -dependent activation of Parkin. However, our data indicated that the Parkin S65A mutant is also autoubiquitinated (Fig. 4b) and that the  $\Delta$ Ubl mutant showed mild translocation defect and impaired substrate degradation (Supplementary Fig. S8). Moreover, if this is the case, the E3 activity of Parkin pathogenic mutants lacking mitochondrial translocation activity but harbouring intact E3 activity *in vitro* (such as K161N and K211N, which are subjected to the Ser65 phosphorylation) should be activated in the cytosol<sup>38</sup>. However, our previous data indicate that K161N and K211N are not activated by CCCP treatment<sup>23</sup>. Thus, it is conceivable that another step is required for depolarised  $\Delta\Psi_m$ -dependent activation of Parkin E3. In addition, the Ubl domain might not only autoinhibit its E3 activity but also contribute to the mitochondrial translocation and the substrate degradation through an as yet unknown mechanism. We believe that an appropriate way to estimate Parkin E3 activity in the context of mitophagy is to evaluate the ubiquitination and degradation of substrates in cells with depolarised  $\Delta\Psi_m$ . Mfn1 is a well-characterised direct substrate of Parkin<sup>32</sup>, and Parkin-dependent poly-ubiquitination modification of Mfn1 can be detected by Western blotting upon  $\Delta\Psi_m$  depolarisation<sup>32,39,40</sup>. Parkin S65A and S65E appear to ubiquitinate Mfn1, as poly-ubiquitinated forms of Mfn1 were observed (Fig. 4b). However, they cannot degrade it effectively, which suggests that the process of substrate degradation is also impaired in these mutants.

Kondapalli *et al.* have also shown that *T. castaneum* PINK1 (TcPINK1) directly phosphorylates human Parkin at Ser65<sup>18</sup>. We confirmed their finding using recombinant TcPINK1 produced from the same construct (Supplementary Fig. S4). The replacement of MBP-Parkin Ser65 with alanine completely abolished PINK1-mediated phosphorylation, indicating that Ser65 is the sole phosphorylation site *in vitro*. However, experiments in cultured cells showed that the replacement of Ser9, Ser10, Ser101 and Ser198 with alanine affects the Ser65 phosphorylation efficiency (Ser9, ~35% reduction; Ser10, ~76% reduction; Ser101, ~65% reduction; Ser198, ~92% reduction) (Fig. 2a). These residues might be priming phosphorylation sites for Ser65 phosphorylation.

Because PINK1 is believed to be activated in the mitochondria, a topological inconsistency arises from our cell-based data that cytosolic Parkin lacking the mitochondrial translocation activity is phosphorylated. Therefore, it is possible that PINK1 indirectly regulates Parkin phosphorylation. One possible explanation for this is the presence of another cytosolic kinase(s) regulated by PINK1 (Fig. 4d). Alternatively, because mitochondria are a dynamic organelle, cytosolic Parkin adjacent to the moving and fragmented mitochondria with depolarised  $\Delta\Psi_m$  might be phosphorylated incidentally. The issue as to whether or not PINK1 directly phosphorylates Parkin in cells remains to be solved.

In conclusion, this study has suggested that PINK1-dependent Parkin phosphorylation at Ser65 accelerates the mitochondrial translocation of Parkin and showed that the introduction of mutations at this site also affects subsequent mitophagy processes. Concurrently, our data provide the possibility that there is an elaborate multi-step mechanism for the mitochondrial translocation of Parkin upon the loss of  $\Delta\Psi_m$  (Fig. 4d), the clarification of which awaits further study.

## Methods

**Antibodies, plasmids and cell lines.** Antibodies used in Western blot analysis were as follows: anti-Parkin (1 : 1,000 and 1 : 5,000 dilution for endogenous and exogenous Parkin, respectively; Cell Signaling Technology, clone PRK8), anti-PINK1 (1 : 1,000 dilution; Novus, BC100-494 or 1 : 1,000 dilution; Cell Signaling Technology, clone D8G3), anti-Mfn1 (1 : 1,000 dilution; Abnova, clone 3C9), anti-VDAC1 (1 : 1,000

dilution; Abcam, Ab15895), anti-Tom20 (1 : 500 dilution; Santa Cruz Biotechnology, FL-145), anti-FLAG-HRP (1 : 2,000 dilution; Sigma-Aldrich, clone M2), anti-GFP (1 : 5,000 dilution; Abcam, ab290), anti-Actin (1 : 10,000 dilution; Millipore, MAb1501), anti-LDH (1 : 1,000 dilution; Abcam, ab7639-1), anti-phospho-GSK3 $\beta$  (1 : 1,000 dilution; Cell Signaling Technology, clone 5B3), anti-GSK3 $\beta$  (1 : 1,000 dilution; Cell Signaling Technology, clone 27C10), and anti-Hsp60 (1 : 10,000 dilution; BD Biosciences, clone 24/Hsp60). Antibodies used in immunocytochemistry were as follows: FITC-conjugated anti-GFP (1 : 1,000 dilution; Abcam, ab6662), anti-Tom20 (1 : 1,000 dilution; Santa Cruz Biotechnology, FL-145), anti-Myc (1 : 500 dilution; Millipore, clone 4A6), anti-p62 (1 : 500 dilution; Progen Biotechnik, GP62-C), anti-Parkin (1 : 1,000 dilution; Cell Signaling Technology, clone PRK8) and anti-proteasome  $\alpha$ 7 (1 : 250; a kind gift of Dr S. Murata at the University of Tokyo). cDNAs for human Parkin, PINK1 and its pathogenic and engineered mutants are as described in previous studies<sup>33,41</sup>. Parkin phospho-mutants were generated by PCR-based mutagenesis followed by sequencing confirmation of the entire gene. PINK1<sup>-/-</sup> MEFs, cultured as previously described<sup>23</sup>, were retrovirally transfected with pMXs-puro harbouring non-tagged PINK1, PINK1-FLAG, non-tagged Parkin, HA-Parkin, GFP-Parkin and related cDNA; transfected cells were then selected with 1  $\mu$ g/ml puromycin. HeLa cells maintained at 37°C in a 5% CO<sub>2</sub> atmosphere in Dulbecco's Modified Eagle's Medium (DMEM) supplemented with 10% FCS and 1x non-essential amino acids (GIBCO) were retrovirally transfected with pMXs-puro harbouring non-tagged Parkin along with pcDNA3Hyg-mSlc7a1-VSVG and pcDNA3Hyg-mSlc7a1-FLAG (a kind gift of Dr N. Fujita at UCSD). Stable cell lines were selected with 1  $\mu$ g/ml puromycin and cloned. Transient transfections of cultured cells were performed using Lipofectamine 2000 (Invitrogen) for plasmids and Lipofectamine RNAiMAX (Invitrogen) for stealth siRNA duplexes (Invitrogen), which were used according to the manufacturer's instructions.

**Tissue culture.** Skin biopsies were obtained from a PARK6 case and a control without mutations in any known PD genes. The study was approved by the ethics committee of Juntendo University, and all participants gave written, informed consent. Dermal primary fibroblasts established from biopsies were cultured in high glucose DMEM supplemented with 10% foetal bovine serum, 1x non-essential amino acids, 1 mM sodium pyruvate (GIBCO), 100  $\mu$ M 2-mercaptoethanol, and 1% penicillin-streptomycin at 37°C in a 5% CO<sub>2</sub> atmosphere.

**Mapping of Parkin phosphorylation sites.** PINK1<sup>-/-</sup> MEFs (6.0  $\times$  10<sup>7</sup>) expressing HA-Parkin and PINK1-FLAG were treated with or without 30  $\mu$ M CCCP for 30 min. HA-Parkin (~500 ng in each) immunopurified with anti-HA-conjugated agarose beads was eluted with 8 M urea buffered with 50 mM Tris-HCl at pH 9.0. Samples from two independent experiments were digested with trypsin or chymotrypsin and analysed by nano-scale liquid chromatography-tandem mass spectrometry (Dionex Ultimate3000 RSLCnano and ABSciex TripleTOF 5600) followed by MASCOT searching and Mass Navigator/PhosPepAnalyzer processing for identification and label-free quantitation, respectively<sup>42</sup>. Determination of phosphosite localisation was performed based on the presence of site-determining ions<sup>43</sup>.

**Phosphorylation assay and mitochondrial fractionation.** PINK1<sup>-/-</sup> MEFs harbouring HA-Parkin along with wild-type or a kinase-dead form of PINK1-FLAG were metabolically labelled with 175  $\mu$ Ci/ml of [<sup>32</sup>P] orthophosphate in phosphate-free DMEM (GIBCO) with 10% FBS at 37°C for 3 hr. The medium was then replaced with fresh DMEM containing 10% FBS. Cells were treated with CCCP for 1.5 hr and were lysed on ice with lysis buffer containing 0.2% NP-40, 50 mM Tris (pH 7.4), 150 mM NaCl and 10% glycerol supplemented with protease inhibitor (Roche Diagnostics) and phosphatase inhibitor (Pierce) cocktails, and HA-Parkin and PINK1-FLAG were immunoprecipitated with anti-HA (Wako Pure Chemical, clone 4B2)- or anti-FLAG (Sigma-Aldrich, clone M2)-conjugated agarose beads. Immunoprecipitates were separated by SDS-PAGE and transferred onto a PVDF membrane. Autoradiography and Western blotting were performed to visualise proteins. Phos-tag Western blotting was performed as previously described<sup>28</sup>. Briefly, phospho-Parkin and phospho-PINK1 were separated on 8% gels containing 50  $\mu$ M Phos-tag. Mitochondrial and cytosolic fractionations were performed as previously described, with some modifications<sup>20</sup>. The cytosolic fractions were further clarified by a second centrifugation at 105,000 g for 60 min to remove residual organelle membranes.

**Immunocytochemical analysis.** Cells plated on 3.5 mm glass-bottom dishes (MatTek) were fixed with 4% paraformaldehyde in PBS and permeabilised with 50  $\mu$ g/ml digitonin for anti-Tom20 and anti-p62 staining or with 0.1% NP-40 for anti- $\alpha$ 7 staining in PBS. Cells were stained with anti-Tom20 or anti- $\alpha$ 7 antibodies in combination with FITC-conjugated anti-GFP antibody and were counterstained with DAPI for nuclei. Cells were imaged using laser-scanning microscope systems (TCS-SP5, Leica or LSM510 META, Carl Zeiss).

**Statistical analysis.** A one-way repeated measures ANOVA was used to determine significant differences between multiple groups unless otherwise indicated. If a significant result was achieved ( $p < 0.05$ ), the means of the control and the specific test group were analysed using the Tukey-Kramer test.

1. Valente, E. M. *et al.* Hereditary early-onset Parkinson's disease caused by mutations in PINK1. *Science* 304, 1158–1160 (2004).

2. Takatori, S., Ito, G. & Iwatsubo, T. Cytoplasmic localization and proteasomal degradation of N-terminally cleaved form of PINK1. *Neurosci Lett* **430**, 13–17 (2008).
3. Beilina, A. *et al.* Mutations in PTEN-induced putative kinase 1 associated with recessive parkinsonism have differential effects on protein stability. *Proc Natl Acad Sci U S A* **102**, 5703–5708 (2005).
4. Silvestri, L. *et al.* Mitochondrial import and enzymatic activity of PINK1 mutants associated to recessive parkinsonism. *Hum Mol Genet* **14**, 3477–3492 (2005).
5. Sim, C. H. *et al.* C-terminal truncation and Parkinson's disease-associated mutations down-regulate the protein serine/threonine kinase activity of PTEN-induced kinase-1. *Hum Mol Genet* **15**, 3251–3262 (2006).
6. Clark, I. E. *et al.* Drosophila pink1 is required for mitochondrial function and interacts genetically with parkin. *Nature* **441**, 1162–1166 (2006).
7. Park, J. *et al.* Mitochondrial dysfunction in Drosophila PINK1 mutants is complemented by parkin. *Nature* **441**, 1157–1161 (2006).
8. Yang, Y. *et al.* Mitochondrial pathology and muscle and dopaminergic neuron degeneration caused by inactivation of Drosophila Pink1 is rescued by Parkin. *Proc Natl Acad Sci U S A* **103**, 10793–10798 (2006).
9. Kitada, T. *et al.* Mutations in the parkin gene cause autosomal recessive juvenile parkinsonism. *Nature* **392**, 605–608 (1998).
10. Imai, Y., Soda, M. & Takahashi, R. Parkin suppresses unfolded protein stress-induced cell death through its E3 ubiquitin-protein ligase activity. *J Biol Chem* **275**, 35661–35664 (2000).
11. Shimura, H. *et al.* Familial Parkinson disease gene product, parkin, is a ubiquitin-protein ligase. *Nat Genet* **25**, 302–305 (2000).
12. Zhang, Y. *et al.* Parkin functions as an E2-dependent ubiquitin-protein ligase and promotes the degradation of the synaptic vesicle-associated protein, CDCrel-1. *Proc Natl Acad Sci U S A* **97**, 13354–13359 (2000).
13. Deas, E. *et al.* PINK1 cleavage at position A103 by the mitochondrial protease PARL. *Hum Mol Genet* **20**, 867–879 (2011).
14. Jin, S. M. *et al.* Mitochondrial membrane potential regulates PINK1 import and proteolytic destabilization by PARL. *J Cell Biol* **191**, 933–942 (2010).
15. Meissner, C., Lorenz, H., Weihofen, A., Selkoe, D. J. & Lemberg, M. K. The mitochondrial intramembrane protease PARL cleaves human Pink1 to regulate Pink1 trafficking. *J Neurochem* **117**, 856–867 (2011).
16. Whitworth, A. J. *et al.* Rhomboid-7 and HtrA2/Omi act in a common pathway with the Parkinson's disease factors Pink1 and Parkin. *Dis Model Mech* **1**, 168–174; discussion 173 (2008).
17. Narendra, D. P. *et al.* PINK1 is selectively stabilized on impaired mitochondria to activate Parkin. *PLoS Biol* **8**, e1000298 (2010).
18. Kondapalli, C. *et al.* PINK1 is activated by mitochondrial membrane potential depolarization and stimulates Parkin E3 ligase activity by phosphorylating Serine 65. *Open Biol* **2**, 120080 (2012).
19. Okatsu, K. *et al.* PINK1 autophosphorylation upon membrane potential dissipation is essential for Parkin recruitment to damaged mitochondria. *Nat Commun* **3**, 1016 (2012).
20. Lazarou, M., Jin, S. M., Kane, L. A. & Youle, R. J. Role of PINK1 binding to the TOM complex and alternate intracellular membranes in recruitment and activation of the E3 ligase Parkin. *Dev Cell* **22**, 320–333 (2012).
21. Vives-Bauza, C. *et al.* PINK1-dependent recruitment of Parkin to mitochondria in mitophagy. *Proc Natl Acad Sci U S A* **107**, 378–383 (2010).
22. Geisler, S. *et al.* PINK1/Parkin-mediated mitophagy is dependent on VDAC1 and p62/SQSTM1. *Nat Cell Biol* **12**, 119–131 (2010).
23. Matsuda, N. *et al.* PINK1 stabilized by mitochondrial depolarization recruits Parkin to damaged mitochondria and activates latent Parkin for mitophagy. *J Cell Biol* **189**, 211–221 (2010).
24. Kawajiri, S. *et al.* PINK1 is recruited to mitochondria with parkin and associates with LC3 in mitophagy. *FEBS Lett* **584**, 1073–1079 (2010).
25. Ziviani, E., Tao, R. N. & Whitworth, A. J. Drosophila parkin requires PINK1 for mitochondrial translocation and ubiquitinates mitofusins. *Proc Natl Acad Sci U S A* **107**, 5018–5023 (2010).
26. Sha, D., Chin, L. S. & Li, L. Phosphorylation of parkin by Parkinson disease-linked kinase PINK1 activates parkin E3 ligase function and NF-kappaB signaling. *Hum Mol Genet* **19**, 352–363 (2010).
27. Kim, Y. *et al.* PINK1 controls mitochondrial localization of Parkin through direct phosphorylation. *Biochem Biophys Res Commun* **377**, 975–980 (2008).
28. Imai, Y. *et al.* The loss of PGAM5 suppresses the mitochondrial degeneration caused by inactivation of PINK1 in Drosophila. *PLoS Genet* **6**, e1001229 (2010).
29. Woodroof, H. I. *et al.* Discovery of catalytically active orthologues of the Parkinson's disease kinase PINK1: analysis of substrate specificity and impact of mutations. *Open Biol* **1**, 110012 (2011).
30. Yamamoto, A. *et al.* Parkin phosphorylation and modulation of its E3 ubiquitin ligase activity. *J Biol Chem* **280**, 3390–3399 (2005).
31. Narendra, D., Tanaka, A., Suen, D. F. & Youle, R. J. Parkin is recruited selectively to impaired mitochondria and promotes their autophagy. *J Cell Biol* **183**, 795–803 (2008).
32. Tanaka, A. *et al.* Proteasome and p97 mediate mitophagy and degradation of mitofusins induced by Parkin. *J Cell Biol* **191**, 1367–1380 (2010).
33. Okatsu, K. *et al.* p62/SQSTM1 cooperates with Parkin for perinuclear clustering of depolarized mitochondria. *Genes Cells* **15**, 887–900 (2010).
34. Narendra, D., Kane, L. A., Hauser, D. N., Fearnley, I. M. & Youle, R. J. p62/SQSTM1 is required for Parkin-induced mitochondrial clustering but not mitophagy; VDAC1 is dispensable for both. *Autophagy* **6**, 1090–1106 (2010).
35. Chan, N. C. *et al.* Broad activation of the ubiquitin-proteasome system by Parkin is critical for mitophagy. *Hum Mol Genet* **20**, 1726–1737 (2011).
36. Wang, X. *et al.* PINK1 and Parkin Target Miro for Phosphorylation and Degradation to Arrest Mitochondrial Motility. *Cell* **147**, 893–906 (2011).
37. Liu, S. *et al.* Parkinson's disease-associated kinase PINK1 regulates Miro protein level and axonal transport of mitochondria. *PLoS Genet* **8**, e1002537 (2012).
38. Matsuda, N. *et al.* Diverse effects of pathogenic mutations of Parkin that catalyze multiple monoubiquitylation in vitro. *J Biol Chem* **281**, 3204–3209 (2006).
39. Gegg, M. E. *et al.* Mitofusins 1 and mitofusins 2 are ubiquitinated in a PINK1/parkin-dependent manner upon induction of mitophagy. *Hum Mol Genet* **19**, 4861–4870 (2010).
40. Rakovic, A. *et al.* Mutations in PINK1 and Parkin impair ubiquitination of Mitofusins in human fibroblasts. *PLoS One* **6**, e16746 (2011).
41. Shiba, K. *et al.* Parkin stabilizes PINK1 through direct interaction. *Biochem Biophys Res Commun* **383**, 331–335 (2009).
42. Iwasaki, M., Sugiyama, N., Tanaka, N. & Ishihama, Y. Human proteome analysis by using reversed phase monolithic silica capillary columns with enhanced sensitivity. *J Chromatogr A* **1228**, 292–297 (2012).
43. Beausoleil, S. A., Villen, J., Gerber, S. A., Rush, J. & Gygi, S. P. A probability-based approach for high-throughput protein phosphorylation analysis and site localization. *Nat Biotechnol* **24**, 1285–1292 (2006).
44. Li, Y. *et al.* Clinicogenetic study of PINK1 mutations in autosomal recessive early-onset parkinsonism. *Neurology* **64**, 1955–1957 (2005).
45. Zhou, C. *et al.* The kinase domain of mitochondrial PINK1 faces the cytoplasm. *Proc Natl Acad Sci U S A* **105**, 12022–12027 (2008).
46. Chaugule, V. K. *et al.* Autoregulation of Parkin activity through its ubiquitin-like domain. *EMBO J* **30**, 2853–2867 (2011).

## Acknowledgements

We thank Drs K. Tanaka, N. Matsuda, K. Okatsu, T. Kitamura, S. Murata, N. Fujita, N. Furuya, M.M.K. Muqit and R.J. Youle for their generous supply of materials; T. Hasegawa and Y. Imaizumi for the preparation of human fibroblasts; and T. Imura for her technical help. This study was supported by the Naito Foundation, the Novartis Foundation, the Grant-in-Aid for Young Scientists (B) from MEXT in Japan (SK-F, YI), the CREST program of JST (NH) and Grant-in-Aid for Scientific Research on Innovative Areas (NH).

## Author contributions

K.S., Y. Imai and N.H. designed the research; K.S., Y. Imai, S.Y., T.K. and Y. Ishihama performed the experiments; S.S. contributed new reagents/analytic tools; K.S. and Y. Imai analysed the data; and Y. Imai and N.H. wrote the paper. K.S. and Y. Imai contributed equally to this work.

## Additional information

Supplementary information accompanies this paper at <http://www.nature.com/scientificreports>

Competing financial interests: The authors declare no competing financial interests.

License: This work is licensed under a Creative Commons Attribution-NonCommercial-NoDerivs 3.0 Unported License. To view a copy of this license, visit <http://creativecommons.org/licenses/by-nc-nd/3.0/>

How to cite this article: Shiba-Fukushima, K. *et al.* PINK1-mediated phosphorylation of the Parkin ubiquitin-like domain primes mitochondrial translocation of Parkin and regulates mitophagy. *Sci. Rep.* **2**, 1002; DOI:10.1038/srep01002 (2012).

## VPS35 Mutation in Japanese Patients with Typical Parkinson's Disease

Maya Ando, MD,<sup>1</sup> Manabu Funayama, PhD,<sup>1,2\*</sup> Yuanzhe Li, MD, PhD,<sup>2</sup> Kenichi Kashihara, MD, PhD,<sup>3</sup> Yoshitake Murakami, MD,<sup>4</sup> Nobutaka Ishizu, MD,<sup>5</sup> Chizuko Toyoda, MD,<sup>6</sup> Katsuhiko Noguchi, MD,<sup>7</sup> Takashi Hashimoto, MD,<sup>8</sup> Naoki Nakano, MD,<sup>9</sup> Ryogen Sasaki, MD, PhD,<sup>10</sup> Yasumasa Kokubo, MD, PhD,<sup>10</sup> Shigeki Kuzuhara, MD, PhD,<sup>11</sup> Kotaro Ogaki, MD,<sup>1</sup> Chikara Yamashita, MD,<sup>1</sup> Hiroyo Yoshino, PhD,<sup>2</sup> Taku Hatano, MD, PhD,<sup>1</sup> Hiroyuki Tomiyama, MD, PhD,<sup>1,12</sup> and Nobutaka Hattori, MD, PhD<sup>1,2,12\*</sup>

<sup>1</sup>Department of Neurology, Juntendo University School of Medicine, Tokyo, Japan

<sup>2</sup>Research Institute for Diseases of Old Age, Graduate School of Medicine, Juntendo University, Tokyo, Japan

<sup>3</sup>Department of Neurology, Okayama Kyokuto Hospital, Okayama, Japan

<sup>4</sup>Department of Neurology, Saiseikai Kurihashi Hospital, Saitama, Japan

<sup>5</sup>Department of Neurology, Saitama National Hospital, Saitama, Japan

<sup>6</sup>Department of Neurology, Jikei Daisan Hospital, Tokyo, Japan

<sup>7</sup>Department of Neurology, Kakio Kinen Hospital, Tokyo, Japan

<sup>8</sup>Hashimoto Clinic, Osaka, Japan

<sup>9</sup>Department of Neurosurgery, Kinki University Hospital, Osaka, Japan

<sup>10</sup>Department of Neurology, Mie University Graduate School of Medicine, Tsu, Mie, Japan

<sup>11</sup>Department of Medical Welfare, Faculty of Health Science, Suzuka University of Medical Science, Suzuka, Mie, Japan

<sup>12</sup>Department of Neuroscience for Neurodegenerative Disorders, Juntendo University School of Medicine, Tokyo, Japan

**ABSTRACT:** Vacuolar protein sorting 35 (*VPS35*) was recently reported to be a pathogenic gene for late-onset autosomal dominant Parkinson's disease (PD), using exome sequencing. To date, *VPS35* mutations have been detected only in whites with PD. The aim of the present study was to determine the incidence and clinical features of Asian PD patients with *VPS35* mutations. We screened 7 reported nonsynonymous missense variants of *VPS35*, including p.D620N, known as potentially disease-associated variants of PD, in 300 Japanese index patients with autosomal dominant PD and 433 patients with sporadic PD (SPD) by direct sequencing or high-resolution melting (HRM) analysis. In addition, we screened 579 controls for the p.D620N mutation by HRM analysis. The p.D620N mutation was detected in 3 patients with autosomal dominant PD (1.0%), in 1 patient with SPD (0.23%), and in no con-

trols. None of the other reported variants of *VPS35* were detected. Haplotype analysis suggested at least 3 independent founders for Japanese patients with p.D620N mutation. Patients with the *VPS35* mutation showed typical tremor-predominant PD. We report Asian PD patients with the *VPS35* mutation. Although *VPS35* mutations are uncommon in PD, the frequency of such mutation is relatively higher in Japanese than reported in other populations. In *VPS35*, p.D620N substitution may be a mutational hot spot across different ethnic populations. Based on the clinical features, *VPS35* should be analyzed in patients with PD, especially autosomal dominant PD or tremor-predominant PD. © 2012 Movement Disorder Society

**Key Words:** Parkinson's disease; *VPS35*; autosomal dominant; hotspot; mutation.

\*Correspondence to: Dr. Manabu Funayama or Prof. Dr. Nobutaka Hattori, Research Institute for Diseases of Old Age, Graduate School of Medicine, Juntendo University, 2-1-1 Hongo, Bunkyo-ku, Tokyo 113-8421, Japan; funayama@juntendo.ac.jp or nhattori@juntendo.ac.jp

**Funding agencies:** This work was supported by Strategic Research Foundation Grant-in-Aid Project for Private Universities, Grants-in-Aid for Scientific Research (80218510 [to N.H.] and 21591098 [to H.T.]), Grant-in-Aid for Young Scientists (22790829 [to M.F.] and 23791003 [to Y.L.]), Grant-in-Aid for Scientific Research on Innovative Areas (23111003 [to N.H.] and 23129506 [to M.F.]) from the Japanese Ministry of Education, Culture, Sports, Science and Technology, and Grant-in-Aid from the Research Committee on Muro Disease (Kii ALS/PDC; 21210301 [to Y.K.]), the Ministry of Health, Labor, and Welfare, and JST, CREST.

**Relevant conflicts of interest/financial disclosures:** Nothing to report. Full financial disclosures and author roles may be found in the online version of this article.

**Received:** 5 March 2012; **Revised:** 11 July 2012; **Accepted:** 17 July 2012  
**Published online in Wiley Online Library (wileyonlinelibrary.com).** DOI: 10.1002/mds.25145

Parkinson's disease (PD) is a neurodegenerative disorder characterized by progressive motor disturbances manifested by tremor, rigidity, akinesia, and postural instability. Neuropathologically, PD is characterized by selective loss of dopaminergic neurons in the substantia nigra and the presence of cytosolic inclusions called Lewy bodies (LBs) in the remaining neurons. The pathogenesis of PD is multifactorial, including genetic–environmental interaction. PD is a common disease in the elderly, with an incidence of about 1%–2% in individuals older than 60 years.<sup>1</sup> Among PD patients, approximately 5%–10% have a positive family history of PD,<sup>2</sup> and among these, the Mendelian forms of PD can contribute to the elucidation of the molecular pathways that lead to the degeneration and death of dopaminergic neurons.

Mutations in the vacuolar protein sorting 35 (*VPS35*) gene have recently been identified in families with autosomal dominant late-onset PD (MIM 601501).<sup>3,4</sup> Patients with *VPS35* mutations present with tremor-predominant dopa-responsive parkinsonism.<sup>3,4</sup> *VPS35*, a key component of the retromer cargo-recognition complex, is thought to associate with sorting cargos into the tubular endosomal network for retrieval to the trans-Golgi network.<sup>5</sup> Therefore, pathogenic mutations of *VPS35* may cause disruption of the retrograde transport system and contribute to dopaminergic neuronal cell death in PD. One missense mutation has been reported to be pathogenic for PD.<sup>3,4</sup> Mutation of c.1858G>A (p.D620N) was identified in 3 Austrian families and 1 family each in Switzerland, the United States, Tunisia, and the United Kingdom, as well as 1 family and 1 patient with sporadic PD (SPD) among Yemenite Jews from Israel.<sup>3,4,6</sup> In addition, several variants, such as p.M57I, p.I241M, p.P316S, and p.R524W, have been reported in Europe and the United States as potentially pathogenic for PD.<sup>3,4</sup>

Although multipopulation screenings for *VPS35* mutations were performed in recent reports, there is still no report of PD patients with *VPS35* mutations of Asian ancestry.<sup>3,4,6–8</sup> In the present study, we screened Japanese patients with autosomal-dominant PD (ADPD), Japanese patients with SPD, and control subjects for mutations of *VPS35*, with a special focus on 7 reported nonsynonymous variants that were found in patients with PD, including the p.D620N. Here, we report 3 families and 1 SPD patient with the p.D620N mutation in *VPS35* and describe their clinical features.

## Patients and Methods

### Subjects

The study was approved by the ethics committee of Juntendo University, and all subjects gave written

informed consent to participate in the genetic research. The study subjects were 308 Japanese patients (300 index patients) with ADPD (age at disease onset [AAO; mean  $\pm$  SD], 51.1  $\pm$  11.7 years; range, 8–83 years; female/male [F/M] ratio, 1.35) and 433 Japanese SPD patients (AAO, 47.2  $\pm$  12.9 years; range, 5–88 years; F/M ratio, 1.09) selected from the gene bank of Juntendo University. Some of the selected subjects had been confirmed negative for *SNCA*, *PARK2*, *PINK1*, *PARK7*, *LRRK2*, and *PLA2G6* mutations.<sup>9–14</sup> From the same gene bank, we also selected 579 healthy Japanese subjects without a family history of parkinsonism (age at sampling, 58.0  $\pm$  9.3 years; range, 23–89 years; F/M ratio, 1.54). The criteria for the diagnosis of PD were adopted by the participating neurologists and were established based on the United Kingdom Parkinson's Disease Society Brain Bank.<sup>15</sup>

### Genetic Analysis

Genomic DNA was extracted from peripheral blood using a standard protocol. Patients with ADPD and SPD were examined for the following 7 variants: p.M57I (exon 3), p.I241M (exon 7), p.P316S (exon 9), p.R524W (exon 13), p.D620N (exon 15), p.A737V (exon 16), and p.L774M (exon 17) of *VPS35* (RefSeq accession number NM\_018206.4). PCR direct sequencing was performed using a BigDye Terminator v1.1 Cycle Sequencing kit and 3130 Genetic Analyzer (Applied Biosystems, Foster City, CA) or 3730 DNA Analyzer (Applied Biosystems). In addition, SPD patients and control subjects were also genotyped for c.1858G>A (p.D620N) mutation by high-resolution melting (HRM) analysis using LightScanner and LCGreen plus (Idaho Technology, Salt Lake City, UT). HRM analysis was performed using a previously described protocol<sup>16</sup> and the following primers: forward, GAGGATGGTTGGTCCTTGAA; reverse, TGCCAATGATCAAGGTGATG. All exons of *VPS35* were also analyzed in patients with the p.D620N mutation using the method described previously.<sup>3</sup>

Haplotype analysis of the *VPS35* flanking region was performed using 3130 Genetic analyzer and GeneMapper software (Applied Biosystems, Foster City, CA). To adjust the size of PCR products, we also genotyped Centre d'Étude du Polymorphisme Humain (CEPH) control samples (1331-01 and 1331-02) for comparison of haplotypes with previously reported patients carrying the p.D620N mutation. The sequences of the PCR primers were reported previously.<sup>3</sup>

## Results

### Detection of p.D620N Mutation

We detected the heterozygous missense p.D620N mutation in 3 unrelated patients with ADPD and 1

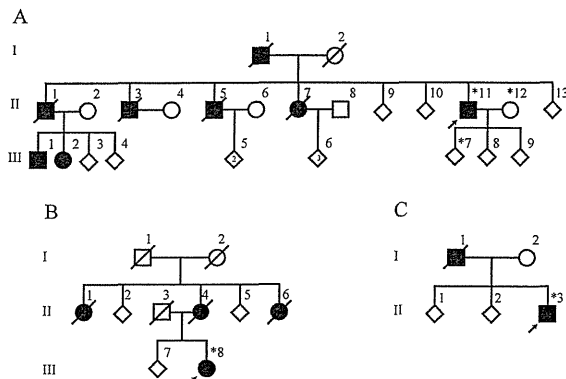


**FIG. 1.** Pedigrees of families with the *VPS35* p.D620N mutation (open symbol, unaffected family member; closed symbol, affected member; arrow, proband; asterisk, individual analyzed for the p.D620N mutation and/or haplotype; forward slash through symbol, deceased individuals; square, male; circle, female; diamond, unspecified sex).

patient with SPD (Fig. 1). The p.D620N has been reported previously as a pathogenic mutation for familial PD.<sup>3,4,6</sup> This mutation was not found in 1158 control chromosomes. Patients carrying the p.D620N mutation did not have any other variants in all exons of *VPS35*. In our population, the incidence of the p.D620N mutation was 1.0% (3 of 300) in ADPD and 0.23% (1 of 433) in SPD. The remaining variants analyzed in this study were not identified in any patients.

Haplotype analysis demonstrated that the Japanese patients with the p.D620N mutation had different genotypes from those of white patients with the same mutation.<sup>3</sup> One disease allele was detected by analyzing patient AII-11 and his relatives. Patients AII-11 and BIII-8 in this study carried at least the same single allele of microsatellites in the flanking region of *VPS35* (Table 1). On the other hand, patients CII-3 and D had a different genotype of D16S3105, with a locus mapped very close to *VPS35*, compared with the disease allele of AII-11 (Table 1, boldface).

**TABLE 1.** Haplotype analysis of *VPS35* p.D620N mutation carriers

Microsatellite	Patient ID			
	AII-11	BIII-8	CII-3	D
D16S401	170	166/170	166/172	166/170
D16S3068	143	141/145	145/147	145/145
D16S753	272	272/268	268/276	264/268
<i>VPS35</i> p.D620N	A	A/G	A/G	A/G
Chr16_45.333M	294	294/298	294/300	294/304
D16S3105	191	191/189	189/193	187/187
Chr16_45.615M	147	147/147	147/145	147/145
Chr16_45.806M	246	246/238	246/244	246/244
Chr16_45.835M	237	237/237	237/237	237/237
Chr16_45.855M	212	212/210	210/210	210/216
D16S3044	195	195/195	195/197	197/197

Both alleles are shown when markers of phase could not be determined.

**TABLE 2.** Clinical features of patients with p.D620N mutation

	Patient ID			
	AII-11	BIII-8	CII-3	D
Age at disease onset (y)	62	55	34	42
Disease duration (y)	15	2	7	21
Resting tremor	+	+	+	+
Bradykinesia	+	+	+	+
Rigidity	+	+	+	+
Gait disturbance	+	-	-	+
Postural instability	+	-	-	+
Clinical response to levodopa	+	+	+	+
Wearing off	+	-	+	+
Asymmetry at onset	+	+	+	+
Orthostatic hypotension	+	-	-	-
Incontinence	+	-	-	-
Urinary urgency	-	-	-	-
Levodopa-induced dyskinesia	+	-	+	+
Sleep benefit	+	-	+	Unknown
Dystonia at onset	-	-	-	-
Hyperreflexia	-	-	-	-
Hallucination	-	-	-	-
Other psychosis	-	-	-	-
Dementia	+	-	-	-
Gaze palsy	-	-	-	-
Brain MRI	WNL	WNL	WNL	WNL
Cardiac MIBG scintigraphy	H/M ratio (E/L), 2.38/2.68; washout ratio, 4.15% <sup>a</sup>	Not performed	Not performed	Not performed

<sup>a</sup>MIBG scintigraphy was performed when AII-11 was 76 years old. WNL, within normal limit; H/M ratio, heart-to-mediastinum ratio; (E/L), early/late stage.

### Clinical Presentation

Table 2 summarizes the clinical features of the 4 *VPS35* mutation-positive patients. Patient AII-11 was a 77-year-old man who developed right upper limb rest tremor at age 62. At age 75, he underwent gastrostomy for progressive dysphagia, then developed cognitive dysfunction without hallucination. Single-photon emission computed tomography of cerebral blood flow showed no reduction in blood flow in the basal ganglia. His father and 4 of 8 siblings were diagnosed with PD (Fig. 1A) and presented levodopa-responsive typical parkinsonism: upper limb tremor and small-step gait. His nephew and niece were also diagnosed with PD, and the nephew developed parkinsonism in his early fifties. Patients BIII-8 and CII-3 both developed upper limb rest tremor at ages 34 and 55, respectively. The mother and aunts of patient BIII-8



and the father of patient CII-3 also developed PD (Fig. 1B, C). Patient D, who developed upper limb rest tremor at age 42, had no family history of PD. She underwent subthalamic nucleus deep brain stimulation (STN-DBS) at age 60 because of disabling motor fluctuation and dyskinesia refractory to pharmacological treatment. All affected patients were born to noncon-sanguineous parents.

## Discussion

*VPS35* has been reported as the pathogenic gene for ADPD, and only 1 mutation, p.D620N, has been reported in several unrelated white families. To our knowledge, there have been no reports of Asian PD patients with *VPS35* mutations.<sup>3,8</sup> Based on this background, we set out in this study to determine the incidence of *VPS35* mutations in Japanese patients with PD. We detected the heterozygous p.D620N mutation of *VPS35* in 3 ADPD families and 1 SPD patient with East Asian ancestry. On the other hand, we could not conclude the pathogenicity of 6 other variants that had been reported as potentially pathogenic for PD because none of the variants was detected in our patients with PD.

The frequency of the p.D620N mutation in Japanese patients was 1.0% in ADPD and 0.23% in SPD. Although the exact frequency among whites is undetermined, the frequency is relatively higher in Japanese patients compared with that reported in previous studies (0%–1.22%).<sup>3,4,6,7,17</sup> Moreover, the frequency in Japanese patients also differs greatly from those of other Asian populations such as Taiwanese patients and mainland Chinese patients (0%).<sup>3,8</sup> Although the mutation frequency was expected to be lower than that of other pathogenic genes for ADPD, such as multiplication of *SNCA*<sup>9,18</sup> and point mutation of *LRRK2*,<sup>19–21</sup> *VPS35* may be one of the most important genes in Japanese PD. Because we screened for only 7 reported variants, we cannot determine the exact frequency of *VPS35* mutations in ADPD; we would need to analyze all 17 exons of *VPS35* in ADPD patients to screen for other variants and to assess the incidence of all disease-associated *VPS35* mutations.<sup>3,4</sup> Furthermore, we would need to perform mutational analysis for SPD patients, in addition to ADPD, to identify Asian population-specific variants, such as *LRRK2* p.G2385R, associated with susceptibility for PD.<sup>19</sup>

Based on haplotype analysis reported in previous studies, the substitution of *VPS35* c.1858G>A (p.D620N) occurs from independent mutational events.<sup>3</sup> We were able to determine the chromosomal phase only in patient AII-11 (family A). The p.D620N mutation possibly shared a common founder between Japanese ADPD families A and B; however, it was inconclusive because the phase of patient BIII-8 was

undetermined. On the other hand, the same p.D620N mutation probably occurred independently in patient CII-3 (family C) and patient D. By genotyping of D16S3105, which is located approximately 1.5 kb centromeric of *VPS35*, there were at least 3 different haplotypes in Japanese because families A and C and patient D (SPD) did not have the same alleles for this microsatellite. To determine the chromosomal phase of families B and C, detailed genetic analyses of other family members are needed in future studies. These results suggest the existence of 3 or more founders in Japanese patients, in addition to the reported white patients with the p.D620N mutation or de novo mutations, indicating that the p.D620N mutation site is a mutational hot spot in *VPS35* across different ethnic populations.

According to previous reports, the average AAO of patients with the *VPS35* mutation was 50–60 years ( $50.6 \pm 7.3$  years),<sup>3</sup> with a distinctive feature of a slightly younger AAO compared with patients with idiopathic PD. In our study, the AAO was nonspecific with a wide range between 30–70 years. Because the family history of patient D was unknown, she was categorized as SPD. With regard to *VPS35* mutation penetrance, it is incomplete from the results of a previous report.<sup>3</sup> Therefore, although the frequency is low, patients with p.D620N mutation could be found among SPD patients.

The clinical symptoms of our patients with *VPS35* mutation closely resembled the idiopathic PD form, with tremor-dominant dopa-responsive parkinsonism. Psychiatric problems were inconspicuous; however, dementia may occur in patients with a long disease course, similar to patient AII-11, who had PD for 15 years. Our patients with *VPS35* mutations had normal brain MRI and cardiac MIBG scintigraphy. There have been no definite pathological mutations of *VPS35* in the spectrum of LB disorders. On the basis of these results, patients with *VPS35* mutation could show comparatively benign disease course without widespread LBs pathology.<sup>22,23</sup>

*VPS35* assembles into the retromer cargo-recognition complex that associates with the cytosolic face of the endosomes. The retromer mediates the retrograde transport of transmembrane cargo from the endosomes to the trans-Golgi network.<sup>5</sup> The p.D620N mutation of *VPS35* might cause impairment of interaction with other components of the retromer complex and impaired retrograde trafficking of recycling proteins,<sup>4</sup> similar to  $\alpha$ -synuclein and *LRRK2*, which are involved in vesicle trafficking.<sup>24,25</sup> Mutations in familial PD genes, including *VPS35*, may cause disruption of intracellular trafficking and lead to neurodegeneration. These findings suggest that impairment of intracellular trafficking systems is associated with the pathogenesis of PD. Although the association between the p.D620N mutation of *VPS35* and PD remains unknown, further functional studies might shed light on the pathogenesis



of VPS35 mutation and the effects of interaction with other known pathogenic gene products on PD.

In conclusion, we have reported Asian PD patients with the VPS35 p.D620N mutation. The p.D620N substitution may be a mutational hot spot across different ethnic populations. The frequency of VPS35 mutation was low in ADPD; however, it is relatively high in Japanese patients compared with that reported in other populations.<sup>3,4,6–8</sup> Based on the clinical features of patients with VPS35 mutation, VPS35 should be analyzed in patients with PD, especially ADPD or tremor-predominant PD. ■

**Acknowledgments:** We thank all the participants in this study.

## References

- Lang AE, Lozano AM. Parkinson's disease. First of two parts. *N Engl J Med* 1998;339:1044–1053.
- Lesage S, Brice A. Parkinson's disease: from monogenic forms to genetic susceptibility factors. *Hum Mol Genet* 2009;18:R48–R59.
- Vilariño-Güell C, Wider C, Ross OA, et al. VPS35 mutations in Parkinson disease. *Am J Hum Genet* 2011;89:162–167.
- Zimprich A, Benet-Pagès A, Struhal W, et al. A mutation in VPS35, encoding a subunit of the retromer complex, causes late-onset Parkinson disease. *Am J Hum Genet* 2011;89:168–175.
- Bonifacino JS, Hurley JH. Retromer. *Curr Opin Cell Biol* 2008;4:427–436.
- Sheerin UM, Charlesworth G, Bras J, et al. Screening for VPS35 mutations in Parkinson's disease. *Neurobiol Aging* 2012;4:838.e1–e5.
- Guella I, Soldà G, Cilia R, et al. The Asp620asn mutation in VPS35 is not a common cause of familial Parkinson's disease. *Mov Disord* 2012;27:800–801.
- Zhang Y, Chen S, Xiao Q, et al. Vacuolar protein sorting 35 Asp620Asn mutation is rare in the ethnic Chinese population with Parkinson's disease. *Parkinsonism Relat Disord* 2012;18:638–640.
- Nishioka K, Hayashi S, Farrer MJ, et al. Clinical heterogeneity of alpha-synuclein gene duplication in Parkinson's disease. *Ann Neurol* 2006;59:298–309.
- Kitada T, Asakawa S, Hattori N, et al. Mutations in the parkin gene cause autosomal recessive juvenile parkinsonism. *Nature* 1998;392:605–608.
- Kumazawa R, Tomiyama H, Li Y, et al. Mutation analysis of the PINK1 gene in 391 patients with Parkinson disease. *Arch Neurol* 2008;65:802–808.
- Tomiyama H, Li Y, Yoshino H, et al. Mutation analysis for DJ-1 in sporadic and familial parkinsonism: screening strategy in parkinsonism. *Neurosci Lett* 2009;455:159–161.
- Tomiyama H, Li Y, Funayama M, et al. Clinicogenetic study of mutations in LRRK2 exon 41 in Parkinson's disease patients from 18 countries. *Mov Disord* 2006;21:1102–1108.
- Yoshino H, Tomiyama H, Tachibana N, et al. Phenotypic spectrum of patients with PLA2G6 mutation and PARK14-linked parkinsonism. *Neurology* 2010;75:1356–1361.
- Hughes AJ, Daniel SE, Kilford L, Lees AJ. Accuracy of clinical diagnosis of idiopathic Parkinson's disease: a clinico-pathological study of 100 cases. *J Neurol Neurosurg Psychiatry* 1992;55:181–184.
- Funayama M, Tomiyama H, Wu RM, et al. Rapid screening of ATP13A2 variant with high-resolution melting analysis. *Mov Disord* 2010;25:2434–2437.
- Lesage S, Condroyer C, Klebe S et al. Identification of VPS35 mutations replicated in French families with Parkinson disease. *Neurology* 2012;78:1449–1450.
- Ibáñez P, Lesage S, Janin S, et al. Alpha-synuclein gene rearrangements in dominantly inherited parkinsonism: frequency, phenotype, and mechanisms. *Arch Neurol* 2009;66:102–108.
- Seki N, Takahashi Y, Tomiyama H, et al. Comprehensive mutational analysis of LRRK2 reveals variants supporting association with autosomal dominant Parkinson's disease. *J Hum Genet* 2011;56:671–675.
- Di Fonzo A, Rohe C, Ferreira J, et al. A frequent LRRK2 gene mutation associated with autosomal dominant Parkinson's disease. *Lancet* 2005;365:412–415.
- Gilks WP, Abou-Sleiman PM, Gandhi S, et al. A common LRRK2 mutation in idiopathic Parkinson's disease. *Lancet* 2005;365:415–416.
- Orimo S, Amino T, Yokochi M, et al. Preserved cardiac sympathetic nerve accounts for normal cardiac uptake of MIBG in PARK2. *Mov Disord* 2005;10:1350–1353.
- Verstraeten A, Wauters E, Crosiers D, et al. Contribution of VPS35 genetic variability to LBD in the Flanders-Belgian population. *Neurobiol Aging* 2012;33:e11–e13.
- Caudle WM, Colebrooke RE, Emson PC, et al. Altered vesicular dopamine storage in Parkinson's disease: a premature demise. *Trends Neurosci* 2008;31:303–308.
- Berwick DC, Harvey K. LRRK2 signaling pathways: the key to unlocking neurodegeneration? *Trends Cell Biol* 2011;21:257–265.



Contents lists available at SciVerse ScienceDirect

## Parkinsonism and Related Disorders

journal homepage: [www.elsevier.com/locate/parkreldis](http://www.elsevier.com/locate/parkreldis)

## LRRK2 I2020T mutation is associated with tau pathology

Sachiko Ujiie<sup>a,b</sup>, Taku Hatano<sup>a,\*</sup>, Shin-ichiro Kubo<sup>a</sup>, Satoshi Imai<sup>a,c</sup>, Shigeto Sato<sup>a</sup>, Toshiki Uchihara<sup>d</sup>, Saburo Yagishita<sup>e</sup>, Kazuko Hasegawa<sup>f</sup>, Hisayuki Kowa<sup>b</sup>, Fumihiko Sakai<sup>g</sup>, Nobutaka Hattori<sup>a</sup><sup>a</sup> Department of Neurology, Juntendo University, School of Medicine, 2-1-1 Hongo, Bunkyo-ku, Tokyo 113-8421, Japan<sup>b</sup> Department of Neurology, Kitasato University, School of Medicine, 1-15-1 Kitasato, Minami-ku, Sagami-hara, Kanagawa 252-0329, Japan<sup>c</sup> Department of Toxicology, Hoshi University, School of Pharmacy and Pharmaceutical Sciences, 2-4-41 Ebara, Shinagawa-ku, Tokyo 142-8501, Japan<sup>d</sup> Department of Neurology, Tokyo Metropolitan Institute for Neuroscience, 2-6 Musashidai, Fuchu, Tokyo 183-8526, Japan<sup>e</sup> Department of Pathology, Kanagawa Rehabilitation Center, 516 Nanasawa, Atsugi, Kanagawa 243-0121, Japan<sup>f</sup> Department of Neurology, National Hospital Organization Sagami-hara National Hospital, 18-1 Sakuradai, Minami-ku, Sagami-hara, Kanagawa 252-0315, Japan<sup>g</sup> Saitama International Headache Center, Saitama Neuropsychiatric Institute, 6-11-1 Honmachihigashi, Saitama Chuo-ku, Saitama 338-0003, Japan

## ARTICLE INFO

## Article history:

Received 19 December 2011

Received in revised form

8 March 2012

Accepted 21 March 2012

## Keywords:

LRRK2

I2020T mutation

Pathology

Tau

PARK8

## ABSTRACT

Mutations in the *leucine-rich repeat kinase 2* (*LRRK2*) gene are the most common cause of autosomal-dominant familial Parkinson's disease (FPD). The variable pathological features of *LRRK2*-linked FPD include Lewy bodies, degeneration of anterior horn cells associated with axonal spheroids, neurofibrillary tangles (NFTs) and TAR DNA-binding protein of 43 kDa (TDP-43) positive inclusion bodies. Furthermore, abnormal hyperphosphorylation of microtubule associated protein tau, in part generated by catalysis of protein kinases, has been reported to be involved in progressive neurodegeneration in a number of diseases, including FPD. Thus, we examined six patients carrying the *LRRK2* I2020T mutation, a pathogenic mutation associated with PARK8, and found abnormal tau phosphorylation depositions in the brainstem. Additionally, we found *LRRK2* I2020T enhanced tau phosphorylation in cultured cells co-expressing *LRRK2*-I2020T and 3 or 4-repeated tau. This is the first report describing the relationship between hyperphosphorylation of tau and *LRRK2* I2020T.

© 2012 Elsevier Ltd. All rights reserved.

## 1. Introduction

Parkinson's disease (PD) is a common neurodegenerative disease, characterized by rigidity, bradykinesia, resting tremor and postural instability. Mutations in *leucine-rich repeat kinase 2* (*LRRK2*) have been identified as the causative gene for PARK8-linked PD [1,2]. *LRRK2*, also known as PARK8, is a large protein of 2527 amino acids, with a molecular weight of approximately 280 kDa. *LRRK2* contains multiple protein domains, including a leucine-rich repeat (LRR) domain, a ROC domain, a COR domain, a MAPKKK domain and a WD40 domain [2,3]. Various intracellular functions of *LRRK2* have been reported, with alterations in its kinase activities thought to be critical for neuronal degeneration [4–7]. Interestingly, the *LRRK2* I2020T mutation is located within the kinase domain and is also associated with altered kinase activity [6,8,9]. However, molecular studies have not shown a robust association between neuronal cell death and altered *LRRK2* kinase activity, and the pathogenic mechanism of the *LRRK2* I2020T mutation remains unknown.

Patients with *LRRK2* mutations show pleomorphic neuropathologies, which are not unique to PD and show overlap with other neurodegenerative diseases. These include nigral degeneration with or without Lewy bodies (LB) [2,10–14], also observed in diffuse LB disease [2,12,13], anterior horn cell degeneration associated with axonal spheroids, similar to amyotrophic lateral sclerosis [2], and neurofibrillary tangles (NFTs), also observed in progressive supranuclear palsy (PSP) [2,11,14,15] and Alzheimer's disease (AD) [2,12,13]. Notably, PD cases with G2019S [15], Y1699C [11] or I1371V [16] *LRRK2* mutations, have shown varied tau pathology. Similarly, Li et al. reported that tau was hyperphosphorylated in brain tissues from *LRRK2*-R1441G overexpressing mice, compared with *LRRK2* wild type (WT) mice [17]. In addition, G2019S overexpressing mice [18] and *Drosophila* [19], exhibited tau alterations including mislocalization and hyperphosphorylation. Therefore, we investigated the relationship between the *LRRK2* I2020T mutation and tau phosphorylation. We examined brain tissue from the Sagami-hara family, a Japanese kindred originally reported to be linked to the PARK8 locus [20], and found abnormally increased deposits of phosphorylated tau in the brainstem. Additionally, we showed that *LRRK2* I2020T enhances tau phosphorylation in cultured cells co-expressing both *LRRK2*-I2020T and 3 or 4-repeated tau.

\* Corresponding author. Tel.: +81 3 38133111; fax: +81 3 58000547.  
E-mail address: [thatano@juntendo.ac.jp](mailto:thatano@juntendo.ac.jp) (T. Hatano).

However, there was no direct interaction between mutant LRRK2 and tau proteins. Our results indicate that the presence of the pathological I2020T mutation causes hyperphosphorylation of tau and may participate in the pathogenesis of PD and other tau-associated neurodegenerative diseases. Our findings contribute to the understanding of PARK8 pathogenesis.

## 2. Material and methods

### 2.1. Subjects

We examined the brains of six patients who came to autopsy. The clinical findings of patients A–E have been reported previously [20,22,23]. In this report patient A represents case 3, B case 4, C case 5, D case 9, E case 10 from the previous report [23]. All patients showed a good response to levodopa developing motor complications in the later stages of their disease, consistent with idiopathic PD. None had marked autonomic or cognitive dysfunction.

Patient F was a 68-year-old female. At 51 years of age, she developed clumsiness in the legs and gait disturbance, and was diagnosed with PD. Treatment with levodopa resulted in a marked improvement of her symptoms. She developed “wearing-off” motor fluctuations at age 57. By 64 years, she had developed visual hallucinations; by age 65, she was unable to walk without assistance. At age 68 of multiple organ failure caused by pneumonia. You have said this already above. This patient was genetically determined to have the I2020T amino acid substitution in LRRK2.

### 2.2. Immunohistochemistry

Autopsy was performed within 6 h after death in each case. Brain sections were fixed in formalin and representative areas were embedded in paraffin and sectioned. Brain sections were stained with hematoxylin–eosin (H&E) for histological examination. For immunohistochemistry, sections of all patients were deparaffinized and incubated with the following primary antibodies: rabbit polyclonal antibody against ubiquitin (Dako; 1:800), and mouse monoclonal antibodies against phosphorylated  $\alpha$ -synuclein (#64; Wako; 1:10,000) and phosphorylation-dependent tau (AT8; Innogenetics, 1:10,000). Primary antibodies were incubated overnight at 4 °C and then visualized by the avidin–biotin–peroxidase complex method. In addition, brain sections were stained with three repeat (3R) or four repeat (4R) tau-specific antibodies (RD3; 1:3000 or RD4; 1:1000 respectively; Upstate) [24], after pretreatment with potassium permanganate and oxalic acid to eliminate non-specific staining [25].

### 2.3. Construct preparation

pRK5-FLAG-LRRK2-WT and LRRK2-I2020T mutant vectors were prepared as described previously [21]. Three or 4 repeat tau cDNA was amplified from human adult brain using reverse transcript PCR and cloned into Myc-pcDNA 3.1(–). The rabbit polyclonal anti-LRRK2 antibody with synthetic peptides at the C-terminal end (2510–2527 aa) of human LRRK2 was generated as described previously [21]. Monoclonal mouse anti-human PHF-tau antibodies (clone AT-180 and clone AT-270), and tau antibody (clone HT-7) were from Innogenetics. Secondary antibodies conjugated to horseradish peroxidase were from GE HealthCare Bio-Sciences.

### 2.4. Cell Culture and transfection

COS-1 cells were grown in Dulbecco's modified Eagle's medium (Sigma–Aldrich) supplemented with 10% fetal bovine serum (Sigma–Aldrich) and 1% penicillin/streptomycin (Invitrogen) under an atmosphere of 5% CO<sub>2</sub> at 37 °C. COS-1 cells were transiently transfected with LRRK2 and tau vectors using FuGENE HD Transfection Reagent (Roche Diagnostics) according to the manufacturer's protocol.

### 2.5. Immunoblotting

After 96 h, cells were lysed in lysis buffer containing 50 mM Tris–HCl (pH 7.4), 150 mM NaCl, 1% nonidet P-40, 0.25% DOC, 400  $\mu$ M Na<sub>3</sub>VO<sub>4</sub>, 400  $\mu$ M EDTA, 1 mM EGTA, 10 mM NaF, 10 mM sodium pyrophosphate and protease inhibitors (Complete Mini, EDTA-free; Roche Diagnostics). To detect LRRK2, the samples were resolved on 3–8% NuPAGE Tris-acetate polyacrylamide gels (Invitrogen) in 1  $\times$  NuPAGE Tris-Acetate SDS running buffer and transferred onto polyvinylidene fluoride (PVDF) membrane. The membranes were blocked for 1 h in PBS containing 0.05% Tween-20 (PBS-T) and 5% non-fat milk (BD Difco) and then incubated overnight at 4 °C with the primary antibody. The membranes were washed with PBS-T three times followed by incubation for 1 h at room temperature with horseradish peroxidase-conjugated anti-rabbit IgG (1:4000) and immunoreactivity assessed by chemiluminescence reaction using Western Lightning ECL (Perkin Elmer–Cetus). To detect tau, samples were resolved on 10% NuPAGE Bis-Tris polyacrylamide gels (Invitrogen) in 1  $\times$  NuPAGE MOPS SDS running buffer and transferred onto PVDF membrane. The membranes were blocked for 1 h in TBS containing 0.05% Tween-20 (TBS-T) and 5%

non-fat milk (BD Difco) and then incubated overnight at 4 °C with the primary antibody. The membranes were washed with TBS-T buffer three times followed by incubation for 1 h at room temperature with horseradish peroxidase-conjugated anti-mouse IgG (1:2000). The remaining steps were as described above. Blots were quantified using Image J software analysis.

### 2.6. Immunoprecipitation

Cell lysates were centrifuged at 15,000  $\times$  g for 20 min at 4 °C and the resulting supernatant fluid was incubated with Anti-FLAG M2 Agarose (Sigma–Aldrich) overnight at 4 °C. The resin was separated by centrifugation, washed three times with lysis buffer and then boiled in Laemmli sample buffer. Finally, each sample was analyzed by SDS-PAGE followed by immunoblotting.

### 2.7. Statistical analysis

Three group comparisons were analyzed by UNI-ANOVA followed by Turkey's multiple comparison tests (SPSS). All values were expressed as mean  $\pm$  SEM. A *P* value less than 5% denoted a statistically significant difference among the groups.

## 3. Results

### 3.1. Variable tau pathology in PD associated with LRRK2 I2020T mutation

A previous pathological study of LRRK2 I2020T patients reported an apparent loss of nigral neurons without LBs, with the exception of one case with LBs. However extensive immunohistochemical analysis of phosphorylated tau was not performed.

The pathological features of patients A–E have been described previously [23]. The additional new patient (patient F) shared neuropathological features with patients A–E, as follows [23]. Macroscopic examination revealed marked discoloration of the substantia nigra (SN) (Fig. 1a), with a well preserved locus coeruleus (LC) (Fig. 1b). This region-specific contrast in neuropathology was confirmed following microscopic examination, with marked neuronal loss, gliosis and extraneuronal melanin present in SN (Fig. 1c), in contrast to well preserved neurons with minimal gliosis in LC (Fig. 1d). Of note, the dorsal motor nucleus of the vagus nerve (DVN) appeared predominantly normal. In addition, we observed Marinesco bodies, ubiquitin-positive intranuclear inclusions, in the surviving neuromelanin-containing SN neurons (Fig. 1e).

Characteristics of the tau-positive lesions are summarized in Table 1. Patient B and E had tau-positive lesions restricted to the brainstem, namely SN, LC and the trochlear nucleus (Fig. 2a). In patients C and D, abnormal phosphorylated tau depositions were observed not only in the brainstem but also in the hippocampus and amygdala. Senile plaques were not found in any regions. In patients A and F, there were no tau-positive lesions. Immunohistochemistry with isoform-specific antibodies, determined that the tau-positive lesions contained both 3R and 4R tau (Fig. 2b, c). Overall, these results show that the I2020T mutation causes autosomal-dominant PD with a pleomorphic pathology, as observed with other LRRK2 mutations.

### 3.2. LRRK2 is associated with hyperphosphorylation of tau

Based on our pathological findings in LRRK2 I2020T patients, we hypothesized that mutant LRRK2 may be involved in hyperphosphorylation of tau. To determine the effect of LRRK2 I2020T on tau phosphorylation, we co-transfected COS-1 cells with LRRK2-WT or I2020T and 4R tau. Levels of phosphorylated tau and total tau were assessed by western blotting using antibodies, which recognize tau phosphorylation, AT-180 at Thr231 and AT-270 at Thr181 (Fig. 3c, d). Neither LRRK2-WT nor I2020T changed expression levels of total tau protein (Fig. 3c, d). However, significantly increased levels of phosphorylated 4R tau were detected in cells with overexpressed LRRK2-I2020T, but not WT (AT-180: 100.0  $\pm$  1.2% [mean  $\pm$  SEM] with WT vs. 118.5  $\pm$  1.5% with I2020T, *p* < 0.001; AT-

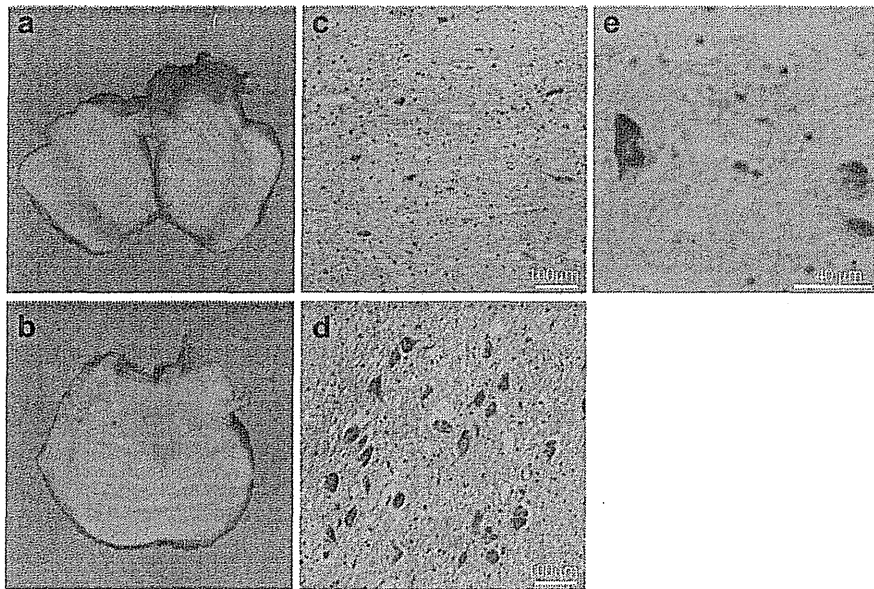


**Fig. 1.** Neuropathology of patient F, a LRRK2 I2020T carrier from the original Japanese Sagamihara family. Marked discoloration of the substantia nigra (SN, a) and relative preservation of locus coeruleus (LC, b). Marked neuronal loss with gliosis in the SN (c, H&E) is in contrast with preserved neurons in LC (d, H&E). Marinesco bodies are abundant in the SN (e, ubiquitin immunostain). Bars: c, d:100  $\mu$ m; e: 40  $\mu$ m.

270:  $93.7 \pm 4.0\%$  with WT vs.  $113.8 \pm 5.3\%$  with I2020T,  $p < 0.001$ ; Fig. 3c, d). Next, we determined if I2020T affects expression levels of phosphorylated 3R tau. LRRK2-I2020T induced a significant, albeit modest, increase in the level of phosphorylated 3R tau protein compared with WT (AT-180:  $94.9 \pm 2.4\%$  with WT vs.  $100.5 \pm 6.5\%$  with I2020T, n.s.; AT-270:  $93.5 \pm 1.2\%$  with WT vs.  $104.1 \pm 2.5\%$  with I2020T,  $p < 0.01$ ; Fig. 3a, b). To investigate further the interaction between LRRK2 and tau, we performed immunoprecipitation experiments. There was no evidence of a direct interaction between either LRRK2-WT or I2020T mutant with 4R tau (Fig. 3e).

#### 4. Discussion

Tau pathology has been identified in the brains of PD patients with LRRK2 mutations, with reports of various forms of tau depositions of, for example PSP-like or AD-like distribution and pattern of age related changes [26,27]. In this study, we identified tau pathology in four patients with LRRK2 I2020T mutation; an

**Table 1**  
Summary of tau pathology in LRRK2 I2020T carriers from the Sagamihara family

	Patient A	Patient B	Patient C	Patient D	Patient E	Patient F
Hippocampus	–	–	+	+	–	–
Meynert	–	–	–	–	+	–
Amygdala	NA	–	–	++	NA	NA
IV	–	+++	++	–	NA	NA
LC	–	+	++	+	+	–
Central gray matter	–	–	++	–	–	–
SN	–	–	+	–	+	–
Braak stage	<1	<1	2	3	<1	<1

The severity and distribution of NFT pathology was estimated using Braak staging (Braak and Braak 1991) (– none; + mild; ++ moderate; +++ severe; n/a not applicable). Tau pathology was observed in 4 out of 6 patients. Two individuals (patient B and E) had tau-positive lesions restricted to the brainstem, with another two individuals (patient C and D), showing tau-positive lesions in the hippocampus as well as the brainstem. The remaining two patients (patient A and F) did not show tau-positive lesions in any brain regions. IV; trochlear nucleus, LC; locus coeruleus, SN; substantia nigra.

increased amount of phosphorylated tau was associated with LRRK2 I2020T mutation compared to wild type in cultured cell models. In addition, we found that affected members of the Sagamihara family display a homogeneous pattern of neuronal loss, namely degeneration of the SN with relative preservation of LC and DVN. This is in sharp contrast to idiopathic PD, where involvement of LC and DVN is observed. We also identified Marinesco bodies in our patients. The presence of Marinesco bodies has been described in other LRRK2-linked PD patients with R1441C [2] and G2019S mutations [14]. Thus, mutant LRRK2 may possibly affect dopaminergic neurons by accelerating the formation of Marinesco bodies.

In contrast to the homogeneity of neuronal degeneration that we observed, deposits of  $\alpha$ -synuclein were confirmed only in patient E, and tau-positive deposits in the brainstem nuclei also varied? among the subjects. In previous reported pathological findings of LRRK2-linked PD, the presence of LBs and tau deposits did not overlap, even in the same family, which is in agreement with our observations in the Sagamihara family. Cookson et al. reported that although clinical features of LRRK2-linked PD were similar to sporadic PD, the pathological findings varied, confounding the correlation between etiology and disease expression [29]. Similarly, all examined members of the Sagamihara family showed typical PD features irrespective of pathological deposits. In addition, we did not find a direct correlation between tau deposits and clinical symptoms. Tau-positive deposits were seen in the

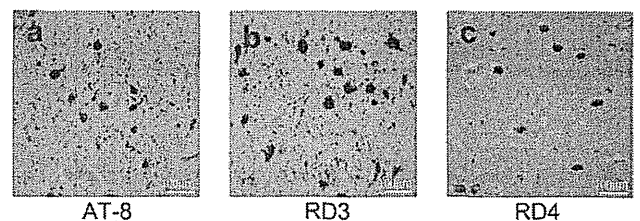


**Fig. 2.** Tau pathology in patient B, a LRRK2 I2020T carrier. Representative immunohistochemical analysis of tau in the trochlear nerve nucleus from Patient B. Sections are labeled with AT8 (a), RD3 (b) and RD4 (c). Bars: c, d:100  $\mu$ m; e: 40  $\mu$ m.

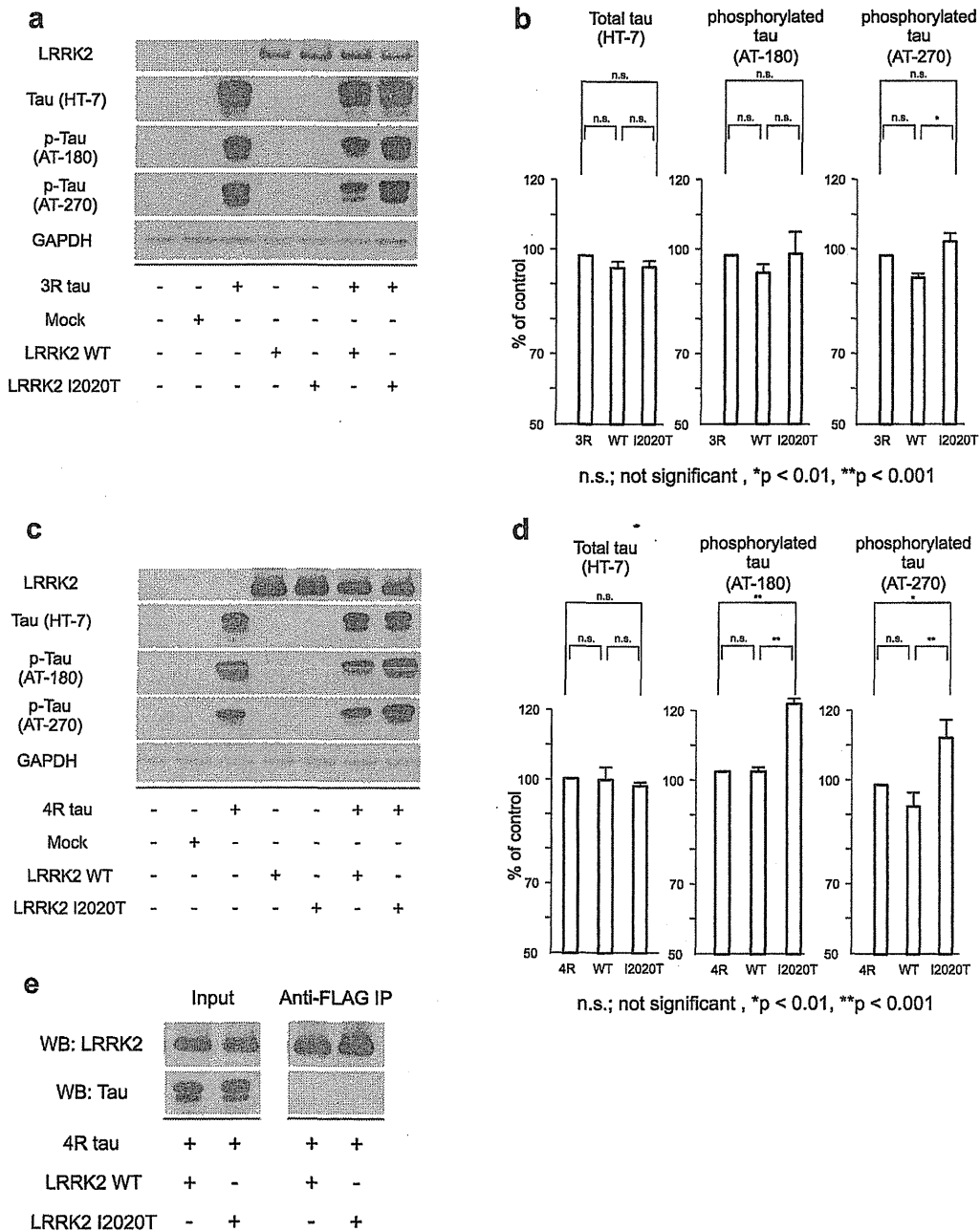


**Fig. 3.** LRRK2-I2020T induces increasing levels of phosphorylated tau compared with LRRK2-WT or mock transfected cells. (a, b) Lysate prepared from COS-1 cells co-expressing 3R tau and LRRK2-WT or I2020T, were subjected to anti-tau (HT-7) or anti-phosphorylated tau (AT-180 and AT-270) immunoblotting. LRRK2-I2020T increased expression levels of phosphorylated tau compared to LRRK2-WT, albeit modestly. (HT-7; 96.3 ± 1.8% with WT vs. 96.5 ± 1.9% with I2020T [mean ± SEM]; n.s., AT-180; 94.9 ± 2.4% with WT vs. 100.5 ± 6.5% with I2020T; n.s., AT-270; 93.5 ± 1.2% with WT vs. 104.1 ± 2.5% with I2020T;  $p < 0.01$ ) (c, d). Lysate prepared from COS-1 cells co-expressing 4R tau and LRRK2-WT or I2020T, were subjected to anti-tau (HT-7) or anti-phosphorylated tau (AT-180 and AT-270) immunoblotting. LRRK2-I2020T significantly increased expression levels of phosphorylated tau compared to LRRK2-WT. (HT-7; 99.7 ± 3.5% with WT vs. 97.8 ± 1.1% with I2020T; n.s. AT-180; 100.0 ± 1.2% with WT vs. 118.5 ± 1.5% with I2020T;  $p < 0.001$ , AT-270; 93.7 ± 4.0% with WT vs. 113.8 ± 5.3% with I2020T;  $p < 0.001$ ). (e) Lysate prepared from COS-1 cells transfected with Myc-4 repeats tau and FLAG-LRRK2-WT or FLAG-LRRK2-I2020T, were subjected to immunoprecipitation with anti-FLAG antibody followed by anti-tau (HT-7) immunoblotting. In the left panel, cell lysates were used to detect the expression of LRRK2 and tau. In the right panel, FLAG-LRRK2 was immunoprecipitated using FLAG antibody. Upper lanes show LRRK2 detected with anti-LRRK2 antibody. Lower lanes show that no bands were obtained with anti-HT-7 antibody. As a result, LRRK2 does not directly interact with 4R tau.

nucleus of the trochlear nerve in patients B and C, neither exhibited ophthalmoparesis. Consistent with these findings, Vitte et al. reported that LRRK2 protein is present throughout the human brain, with intense immunoreactivity in the neurons of several midbrain nuclei, including the nucleus of the trochlear nerve [28].

We then demonstrated the association between LRRK2 and tau hyperphosphorylation by using cultured cell models. Compared to LRRK2-WT or mock transfected, overexpression of LRRK2-I2020T in cultured cells resulted in increased levels of phosphorylated tau proteins. Furthermore, this increase in phosphorylated tau was



associated with upregulation of both 3R and 4R tau isoforms. These findings could provide support for abnormal hyperphosphorylated tau deposition in the pathological findings of patients with *LRRK2 I2020T* mutation.

Based on neuropathological findings and cultured cell models, we hypothesized that *LRRK2* is able to enhance tau phosphorylation. Our immunoprecipitation studies showed no evidence of a direct interaction between either *LRRK2*-WT or *I2020T* mutant with tau, indicating that tau phosphorylation by *LRRK2*-*I2020T* involves the association of an intermediate, genetic, or environmental factor. Smith et al. also reported that *LRRK2* failed to bind tau protein [30]. Furthermore, *LRRK2* mutations have been reported to be associated with tau hyperphosphorylation without direct interaction in animal models. Li et al. reported that tau is hyperphosphorylated in brain tissues from *LRRK2*-R1441G overexpressing mice compared with *LRRK2*-WT mice [17]. Mice and *Drosophila* overexpressing *LRRK2*-G2019S also exhibited tau alterations, including mislocalization and increased tau phosphorylation [18,19]. Therefore, we believe that *LRRK2* mutations can be involved in the tau phosphorylation pathway.

How *LRRK2* can participate in the tau phosphorylation pathway remains unclear. In addition, we failed to find that these abnormal tau deposits have any apparent spatial correlation with our observed region-specific neuronal degeneration in the Sagami-hara family. Therefore, future work will need to evaluate the association between neurodegeneration and the tau hyperphosphorylation due to *LRRK2 I2020T* mutation.

#### Conflicts of interest

None declared.

#### Acknowledgements

We thank Shinji Saiki, Yukiko Takata-Usami, Kenneth Isamu Tsukaguchi, Sumihiro Kawajiri, Hiroto Eguchi, Kahori Shiba-Fukushima and Yoko Imamichi (Juntendo University). This work was supported in part by grants for the Scientific Research Priority Areas (to N.H.), the Scientific Research B (to N.H.), the Scientific Research C (to T.U. and S.K.), the Young Scientists B (to T.H.) from the Japanese Ministry of Education, Culture, Sports, Science and Technology; the core research for evolutionary science and technology in the Japan Science and Technology (to N.H.); and the 'Research for the Future' program from the Japan Society for Promotion of Science; a Takeda Science Foundation (to S.K.); Mitsui Life Social Welfare Foundation (T.U.); and Tokyo Metropolitan Organization for Medical Research (T.U.).

#### References

- Paisan-Ruiz C, Jain S, Evans EW, Gilks WP, Simon J, van der Brug M, et al. Cloning of the gene containing mutations that cause PARK8-linked Parkinson's disease. *Neuron* 2004;44:595–600.
- Zimprich A, Biskup S, Leitner P, Lichtner P, Farrer M, Lincoln S, et al. Mutations in *LRRK2* cause autosomal-dominant parkinsonism with pleomorphic pathology. *Neuron* 2004;44:601–7.
- Mata IF, Wedemeyer WJ, Farrer MJ, Taylor JP, Gallo KA. *LRRK2* in Parkinson's disease: protein domains and functional insights. *Trends Neurosci* 2006;29:286–93.
- Greggio E, Jain S, Kingsbury A, Bandopadhyay R, Lewis P, Kaganovich A, et al. Kinase activity is required for the toxic effects of mutant *LRRK2*/dardarin. *Neurobiol Dis* 2006;23:329–41.
- West AB, Moore DJ, Biskup S, Bugayenko A, Smith WW, Ross CA, et al. Parkinson's disease-associated mutations in leucine-rich repeat kinase 2 augment kinase activity. *Proc Natl Acad Sci U S A* 2005;102:16842–7.
- West AB, Moore DJ, Choi C, Andrabi SA, Li X, Dikeman D, et al. Parkinson's disease-associated mutations in *LRRK2* link enhanced GTP-binding and kinase activities to neuronal toxicity. *Hum Mol Genet* 2007;16:223–32.
- Smith WW, Pei Z, Jiang H, Dawson VL, Dawson TM, Ross CA. Kinase activity of mutant *LRRK2* mediates neuronal toxicity. *Nat Neurosci* 2006;9:1231–3.
- Gloekner CJ, Kinki N, Schumacher A, Braun RJ, O'Neill E, Meitinger T, et al. The Parkinson disease causing *LRRK2* mutation I2020T is associated with increased kinase activity. *Hum Mol Genet* 2006;15:223–32.
- Imai Y, Gehrke S, Wang HQ, Takahashi R, Hasegawa K, Oota E, et al. Phosphorylation of 4E-BP by *LRRK2* affects the maintenance of dopaminergic neurons in *Drosophila*. *EMBO J* 2008;27:2432–43.
- Gilks WP, Abou-Sleiman PM, Gandhi S, Jain S, Singleton A, Lees AJ, et al. A common *LRRK2* mutation in idiopathic Parkinson's disease. *Lancet* 2005;365:415–6.
- Khan NL, Jain S, Lynch JM, Pavese N, Abou-Sleiman P, Holton JL, et al. Mutations in the gene *LRRK2* encoding dardarin (PARK8) cause familial Parkinson's disease: clinical, pathological, olfactory and functional imaging and genetic data. *Brain* 2005;128:2786–96.
- Ross OA, Toft M, Whittle AJ, Johnson JL, Papapetropoulos S, Mash DC, et al. *Lrrk2* and Lewy body disease. *Ann Neurol* 2006;59:388–93.
- Giasson BI, Covy JP, Bonini NM, Hurtig HI, Farrer MJ, Trojanowski JQ, et al. Biochemical and pathological characterization of *Lrrk2*. *Ann Neurol* 2006;59:315–22.
- Gaig C, Marti MJ, Ezquerro M, Rey MJ, Cardozo A, Tolosa E. G2019S *LRRK2* mutation causing Parkinson's disease without Lewy bodies. *J Neurol Neurosurg Psychiatry* 2007;78:626–8.
- Rajput A, Dickson DW, Robinson CA, Ross OA, Dachselt JC, Lincoln SJ, et al. Parkinsonism, *Lrrk2* G2019S, and tau neuropathology. *Neurology* 2006;67:1506–8.
- Giordana MT, D'Agostino C, Albani G, Mauro A, Di Fonzo A, Antonini A, et al. Neuropathology of Parkinson's disease associated with the *LRRK2* Ile1371Val mutation. *Mov Disord* 2007;22:275–8.
- Li Y, Liu W, Oo TF, Wang L, Tang Y, Jackson-Lewis V, et al. Mutant *LRRK2*(R1441G) BAC transgenic mice recapitulate cardinal features of Parkinson's disease. *Nat Neurosci* 2009;12:826–8.
- Melrose HL, Dachselt JC, Behrouz B, Lincoln SJ, Yue M, Hinkle KM, et al. Impaired dopaminergic neurotransmission and microtubule-associated protein tau alterations in human *LRRK2* transgenic mice. *Neurobiol Dis* 2010;40:503–17.
- Lin CH, Tsai PI, Wu RM, Chien CT. *LRRK2* G2019S mutation induces dendrite degeneration through mislocalization and phosphorylation of tau by recruiting autoactivated GSK3beta. *J Neurosci* 2010;30:13138–49.
- Funayama M, Hasegawa K, Kowa H, Saito M, Tsuji S, Obata F. A new locus for Parkinson's disease (PARK8) maps to chromosome 12p11.2–q13.1. *Ann Neurol* 2002;51:296–301.
- Hatano T, Kubo SI, Imai S, Maeda M, Ishikawa K, Mizuno Y, et al. Leucine-rich repeat kinase 2 associates with lipid rafts. *Hum Mol Genet* 2007;16:678–90.
- Funayama M, Hasegawa K, Ohta E, Kawashima N, Komiyama M, Kowa H, et al. An *LRRK2* mutation as a cause for the parkinsonism in the original PARK8 family. *Ann Neurol* 2005;57:918–21.
- Hasegawa K, Stoessl AJ, Yokoyama T, Kowa H, Wszolek ZK, Yagishita S. Familial parkinsonism: study of original Sagami-hara PARK8 (I2020T) kindred with variable clinicopathologic outcomes. *Parkinsonism Relat Disord* 2009;15:300–6.
- de Silva R, Lashley T, Gibb G, Hanger D, Hope A, Reid A, et al. Pathological inclusion bodies in tauopathies contain distinct complements of tau with three or four microtubule-binding repeat domains as demonstrated by new specific monoclonal antibodies. *Neuropathol Appl Neurobiol* 2003;29:288–302.
- Uchihara T, Nakamura A, Shibuya K, Yagishita S. Specific Detection of pathological three-repeat tau after pretreatment with potassium permanganate and oxalic acid in PSP/CBD brains. *Brain Pathol* 2011;21:180–8.
- Gaig C, Ezquerro M, Marti MJ, Valdeoriola F, Munoz E, Llado A, et al. Screening for the *LRRK2* G2019S and codon-1441 mutations in a pathological series of parkinsonian syndromes and frontotemporal lobar degeneration. *J Neurol Sci* 2008;270:94–8.
- Taymans JM, Cookson MR. Mechanisms in dominant parkinsonism: the toxic triangle of *LRRK2*, alpha-synuclein, and tau. *Bioessays* 2010;32:227–35.
- Vitte J, Traver S, Maues De Paula A, Lesage S, Rovelli G, Corti O, et al. Leucine-Rich repeat kinase 2 is associated with the Endoplasmic Reticulum in dopaminergic neurons and Accumulates in the core of Lewy bodies in Parkinson disease. *J Neuropathol Exp Neurol* 2010;69:959–72.
- Cookson MR, Hardy J, Lewis PA. Genetic neuropathology of Parkinson's disease. *Int J Clin Exp Pathol* 2008;1:217–31.
- Smith WW, Pei Z, Jiang H, Moore DJ, Liang Y, West AB, et al. Leucine-rich repeat kinase 2 (*LRRK2*) interacts with parkin, and mutant *LRRK2* induces neuronal degeneration. *Proc Natl Acad Sci U S A* 2005;102:18676–81.

Brief communication

## Analysis of *C9orf72* repeat expansion in 563 Japanese patients with amyotrophic lateral sclerosis

Kotaro Ogaki<sup>a</sup>, Yuanzhe Li<sup>b</sup>, Naoki Atsuta<sup>c</sup>, Hiroyuki Tomiyama<sup>a,d</sup>, Manabu Funayama<sup>a,b</sup>, Hazuki Watanabe<sup>c</sup>, Ryoichi Nakamura<sup>c</sup>, Hideo Yoshino<sup>e</sup>, Seiji Yato<sup>f</sup>, Asako Tamura<sup>g</sup>, Yutaka Naito<sup>g,h</sup>, Akira Taniguchi<sup>g</sup>, Koji Fujita<sup>i</sup>, Yuishin Izumi<sup>i</sup>, Ryuji Kaji<sup>i</sup>, Nobutaka Hattori<sup>a,b,d,\*\*</sup>, Gen Sobue<sup>c,\*</sup>, Japanese Consortium for Amyotrophic Lateral Sclerosis research (JaCALS)

<sup>a</sup> Department of Neurology, Juntendo University School of Medicine, Tokyo, Japan

<sup>b</sup> Research Institute for Diseases of Old Age, Juntendo University School of Medicine, Tokyo, Japan

<sup>c</sup> Department of Neurology, Nagoya University Graduate School of Medicine, Nagoya, Japan

<sup>d</sup> Department of Neuroscience for Neurodegenerative Disorders, Juntendo University School of Medicine, Tokyo, Japan

<sup>e</sup> Setagaya Neurological Hospital, Tokyo, Japan

<sup>f</sup> Sayama Neurological Hospital, Sayama, Japan

<sup>g</sup> Department of Neurology, Mie University Graduate School of Medicine, Tsu, Japan

<sup>h</sup> Department of Neurology, Ise Red Cross Hospital, Ise, Japan

<sup>i</sup> Department of Clinical Neuroscience, Institute of Health Biosciences, the University of Tokushima Graduate School, Tokushima, Japan

Received 25 March 2012; received in revised form 20 May 2012; accepted 20 May 2012

### Abstract

Recently, a hexanucleotide repeat expansion in *C9orf72* was identified as the most common cause of both sporadic and familial amyotrophic lateral sclerosis (ALS) and frontotemporal dementia in Western populations. We analyzed 563 Japanese patients with ALS (552 sporadic and 11 familial) using fluorescent fragment-length analysis of *C9orf72* and repeat-primed polymerase chain reaction analysis. Haplotype analysis was performed for 42 single nucleotide polymorphisms in patients with *C9orf72* repeat expansion. *C9orf72* repeat expansion was found in 2 patients with sporadic ALS (2/552 = 0.4%) and no patients with familial ALS (0/11 = 0%). In the probands' families, 1 primary progressive aphasia patient and 1 asymptomatic 76-year-old individual exhibited *C9orf72* repeat expansion. All of the patients with the *C9orf72* repeat expansion carried the 20-single nucleotide polymorphism consensus risk haplotype. The frequency of the *C9orf72* repeat expansion among Japanese patients is much lower than in Western populations. The existence of a 76-year-old asymptomatic carrier supported the notion of incomplete penetrance. The *C9orf72* mutation should be analyzed in sporadic ALS patients after determining their family histories not only of frontotemporal dementia but also of primary progressive aphasia.

© 2012 Elsevier Inc. All rights reserved.

**Keywords:** Amyotrophic lateral sclerosis; *C9orf72*; Incomplete penetrance; Sporadic; Aphasia; Frontotemporal dementia

### 1. Introduction

Amyotrophic lateral sclerosis (ALS) is a neurodegenerative disorder that primarily affects motor neurons in the spinal cord, brain stem, and cerebral cortex, typically leading to death within a few years. Five to ten percent of ALS cases are familial, and the remaining cases are believed to be sporadic (Valdmanis et al., 2009). A number of genes causing ALS with a dominant mode of inheritance have

\* Corresponding author at: Department of Neurology, Nagoya University Graduate School of Medicine, 65 Tsurumai-cho, Showa-ku, Nagoya 466 8550, Japan. Tel.: +81 52 744 2385; fax: +81 52 744 2384.

E-mail address: sobueg@tsuru.med.nagoya-u.ac.jp (G. Sobue).

\*\* Alternate corresponding author at: Department of Neurology, Juntendo University School of Medicine, 2-1-1 Hongo, Bunkyo, Tokyo 113–8421, Japan. Tel.: +81 3 5802 1073; fax: +81 3 5800 0547.

E-mail address: nhattori@juntendo.ac.jp (N. Hattori).



been discovered, such as *SOD1*, *TARDBP*, *FUS*, *VAPB*, *ANG*, *VCP*, *OPTN* (Ticozzi et al., 2011), and *UBQLN2* (Deng et al., 2011). Moreover, there is increasing clinical and pathological evidence for the hypothesis that ALS and frontotemporal dementia (FTD) constitute an overlapping continuum of diseases (Lomen-Hoerth et al., 2002; Neumann et al., 2006). Recently, the expansion of a noncoding GGGGCC hexanucleotide repeat in the *C9orf72* gene has been reported to be a major cause of both ALS and FTD (DeJesus-Hernandez et al., 2011; Gijselinck et al., 2012; Renton et al., 2011) and the most common genetic abnormality in familial and sporadic forms of both ALS and FTD, particularly in Western populations (Chiò et al., 2012; DeJesus-Hernandez et al., 2011; Gijselinck et al., 2012; Renton et al., 2011; Sabatelli et al., 2012; Stewart et al., 2012). In the present study, we describe the incidence and demographic and clinical features associated with the *C9orf72* mutation in a large cohort of Japanese ALS patients. We also perform haplotype analysis to investigate whether Japanese patients have the same risk haplotype as European patients (Gijselinck et al., 2012; Laaksovirta et al., 2010; Mok et al., 2012).

## 2. Methods

### 2.1. Subjects

We obtained a total of 760 DNA samples from the Japanese Consortium for Amyotrophic Lateral Sclerosis Research (JaCALS; Appendix A). A total of 563 (11 familial and 552 sporadic) patients were diagnosed with ALS according to the El Escorial revised criteria (Brooks et al., 2000) and classified as bulbar-onset, spinal-onset, FTD-ALS, or other (see Supplementary Table 1 for details). We had determined the family histories of ALS but not FTD or primary progressive aphasia (PPA) in all of the patients when they were enrolled as patients with sporadic ALS (SALS). We recruited 197 control subjects, none of whom had a medical or family history of neurodegenerative disorders. The mean age at onset of the patients with ALS was  $60.4 \pm 11.7$  years (range 20–86), and the mean age at sampling of the controls was  $60.6 \pm 10.3$  years (range 26–83). All of the subjects were unrelated Japanese individuals. Written informed consent was obtained from all of the subjects. The ethical committees at the participating institutions approved this study.

### 2.2. Fluorescent fragment-length analysis of *C9orf72* and repeat-primed PCR analysis

The normal repeat number of the GGGGCC hexanucleotide was determined in all of the patients and control subjects using genotyping primers, as previously described (DeJesus-Hernandez et al., 2011). To provide a qualitative assessment of the presence of *C9orf72* repeat expansions, we performed repeat-primed polymerase chain reaction

(PCR), as previously described (DeJesus-Hernandez et al., 2011).

### 2.3. Haplotype analysis

We genotyped 42 single nucleotide polymorphisms (SNPs) across 232 kilobase of Chromosome 9p21, which were first described as the founder haplotype in the Finnish ALS population (Laaksovirta et al., 2010), using primers (Supplementary Table 2) to determine whether our Japanese patients carried the haplotype associated with a risk of ALS. These 42 SNPs included the 20-SNP consensus risk allele that had recently been detected in genome-wide association studies in several populations (Mok et al., 2012). We also performed haplotype analysis with 4 microsatellites (D9S1121, D9S169, D9S270, and D9S104) flanking the *C9orf72* GGGGCC repeat, as previously described (Gijselinck et al., 2012) (Fig. 1).

## 3. Results

### 3.1. Detection of *C9orf72* repeat expansion

The *C9orf72* repeat expansion was found in 2 of 522 Japanese patients ( $2/522 = 0.4\%$ ) with SALS and none of the 11 patients ( $0/11 = 0\%$ ) with familial ALS (FALS) using repeat-primed PCR (Table 1). Patient A-I with a *C9orf72* mutation was classified as SALS in this study, but after detecting the mutation, we found that patient A-II (a brother of patient A-I) developed aphasia and dementia and had a *C9orf72* mutation (Fig. 1). The average repeat number based on fluorescent fragment-length analysis was  $3.65 \pm 2.43$  (range 2–13 repeats) in 561 ALS patients without the *C9orf72* mutation. A subsequent analysis of 197 healthy controls did not detect any *C9orf72* mutation. The average repeat number was  $3.69 \pm 2.46$  (range 2–14 repeats) in the 197 controls. The mean age at disease onset in patients with *C9orf72* mutation, including patient A-II, was  $64.7 \pm 6.1$  years (range 57–72). The genotypes of all individuals with the *C9orf72* mutation were detected for the 20 SNPs spanning a 140-kilobase segment concordant with the recently identified risk haplotype on chromosome 9p (Mok et al., 2012) and 24 or 25 consecutive SNPs in the 42-SNP Finish risk haplotype (Laaksovirta et al., 2010) (Fig. 1, Supplementary Table 3).

### 3.2. Clinical presentations of individuals with *C9orf72* mutation

#### 3.2.1. Patient A-I (family A)

Patient A-I was a 65-year-old man who reported weakness in the left leg. The weakness progressed, and he developed fasciculation. At age 66, a neurological examination revealed dementia. His Mini Mental State Examination score was 23/30, and his Frontal Assessment Battery score was 13/18. He also exhibited dysarthria and weakness, atrophy, and fasciculation in the tongue and all 4 modalities. His tendon reflexes were diminished, and the plantar re-

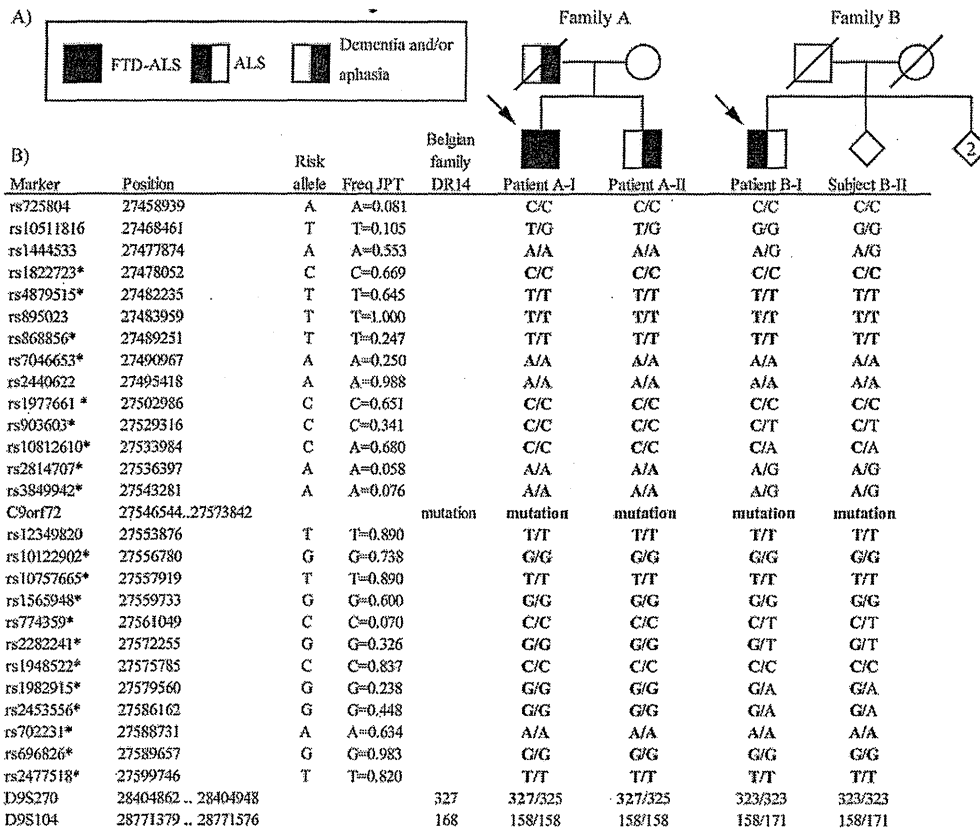


Fig. 1. (A) The pedigrees of the 2 families with *C9orf72* repeat expansion. To maintain confidentiality, several unaffected individuals who died early in families A and B are not shown. Probands are indicated by arrows. (B) The genotyping data of the single nucleotide polymorphisms (SNPs) and microsatellites. Twenty SNPs, which comprised a recently identified consensus risk haplotype (Mok et al., 2012), are shown with an asterisk. See Supplementary Table 3 for details of the analyses of 42 SNPs (Laaksovirta et al., 2010) and microsatellites (Gijssels et al., 2012). Alleles possibly shared between our subjects and patients in Western populations are shown in bold. The genotypes of all 4 subjects with respect to the 20 SNPs were found to be concordant with the risk haplotype (Mok et al., 2012). All of the positions of SNPs and microsatellites were from NC\_000009.11. Abbreviations: ALS, amyotrophic lateral sclerosis; Freq JPT, Frequency in Japanese in Tokyo from International HapMap project (International HapMap Consortium, 2003); FTD, frontotemporal dementia.

sponse was extensor on the left. He had neither dysphagia nor dyspnea. No sensory abnormalities were noted. Extensive screening for causes of motor neuropathy was negative. The diagnosis was clinically probable ALS-laboratory supported (Brooks et al., 2000) and FTD-ALS.

### 3.2.2. Patient A-II (family A)

This patient was a 57-year-old man who presented with difficulty speaking. He was believed to have suffered from a mental disease after being imprisoned because of his involvement in a fatal car accident. At age 64, he was severely dysfluent and could barely speak. Logoclonia was particularly prominent. However, he did not exhibit any violent behavior or other behavioral abnormalities. He also did not display any clinical features of motor neuron disease. Brain magnetic resonance imaging revealed severe frontotemporal lobar atrophy. PPA was considered the most likely diagnosis.

### 3.2.3. Patient B-I (family B)

Patient B-I was a 72-year-old man who presented with gait disturbance and weakness in the proximal lower extremity muscle. His family history was negative for motor neuron disease and dementia (Fig. 1). The muscle weakness and atrophy progressed and spread to the other parts of his body despite treatment with intravenous gamma globulin. At age 74, he could not roll over while sleeping. A neurological examination showed marked muscle atrophy in his arms and shoulders and prominent fasciculation in his legs. The deep tendon reflexes were decreased in his limbs, and he had no pathological reflexes. Sensations in all 4 modalities were intact. At age 75, he developed dyspnea and dysphagia and started noninvasive positive pressure ventilation and intravenous hyperalimentation. He died of respiratory insufficiency at age 76. An autopsy was not performed. The diagnosis was clinically suspected ALS (Brooks et al., 2000).

Table 1  
Frequencies of ALS patients with *C9orf72* and *SOD1* mutations in different countries

Study	Population	<i>C9orf72</i>			<i>SOD1</i>	
		Familial ALS	Sporadic ALS	Mean AAO (range), years	Familial ALS	Sporadic ALS
This study, 2012	Japanese (JaCALS)	0% (0/11)	0.4% (2/552)	64.7 (57–72)	NA	NA
Akimoto et al. (2011)	Japanese (JaCALS)	NA	NA	NA	NA	1.6% (4/255)
DeJesus-Hernandez et al. (2011)	Mixed <sup>a</sup>	23.5% (8/34)	4.1% (8/195)***	54.5 (41–72)	11.8% (4/34)	0% (0/195)
Renton et al. (2011)	Finish	46.4% (52/112)**	21.0% (61/290)***	53 (30–71)	NA	NA
Gijssels et al. (2012)	Flanders-Belgian	46.7% (7/15)*	4.9% (6/122)***	54.5 (38–64)	0% (0/16)	0% (0/125)
Stewart et al. (2012)	Unknown <sup>b</sup>	27.4% (17/62)	3.6% (6/169)**	58.2 (39–82)	Total 8.2% (19/231)	
Byrne et al. (2012)	Ireland	40.8% (20/49)*	4.9% (19/386)***	56.3 (NA)	Total 0% (0/191)	
Cooper-Knock et al. (2012)	Northern England	42.9% (27/63)*	7.0% (35/500)***	57.3 (27–74)	Total 2.5% (14/563)	
Chiò et al. (2012)	Italian	37.5% (45/120)*	NA	59.0 (NA–80)	0% (0/141)	NA
	Sardinian	57.1% (12/21)**	NA	60.4 (NA)	NA	NA
	German	22.0% (9/41)	NA	56.4 (NA)	NA	NA
Majounie et al. (2012)	England	45.9% (45/98)**	6.8% (62/916)***	NA	NA	NA
	German	21.7% (15/69)	5.2% (22/421)***	NA	NA	NA
	Italian	37.8% (34/90)*	4.1% (19/465)***	NA	NA	NA
	Sardinian	57.9% (11/19)**	7.8% (10/129)***	NA	NA	NA
	USA White	US total 36.2% (59/163)*	5.4% (48/890)***	NA	NA	NA
	USA Hispanic		8.3% (6/72)***	NA	NA	NA
	USA Black		4.1% (2/49)	NA	NA	NA
	Australian	NA	5.3% (14/263)***	NA	NA	NA
	Israeli	21.4% (3/14)	NA	NA	NA	NA
	Indian	NA	0% (0/31)	NA	NA	NA
	Asian	5.0% (1/20)	0% (0/238)	NA	NA	NA
	Pacific islander/Guam	NA	0% (0/90)	NA	NA	NA
	Sabatelli et al. (2012)	Italian	NA	3.7% (60/1624)***	58.6 (49–65)	NA
Sardinian		NA	6.8% (9/133)***	62.9 (58–63)	NA	NA

Key: AAO, age at onset; ALS, amyotrophic lateral sclerosis; JaCALS, Japanese Consortium of Amyotrophic Lateral Sclerosis Research; NA, not available.

<sup>a</sup> Mixed included 229 ALS patients from Mayo Clinic, Florida: White (212), Asian (1), Pacific Islander (1), and Black or African American (15).

<sup>b</sup> Unknown included 231 ALS patients from the ALS Clinic of Vancouver Coastal Health and the University of British Columbia (Vancouver General Hospital and GF Strong Rehabilitation Centre sites).

\*  $p < 0.05$ , compared with our results (2-tailed, Yates's  $\chi^2$  test).

\*\*  $p < 0.01$ , compared with our results (2-tailed, Yates's  $\chi^2$  test).

\*\*\*  $p < 0.001$  compared with our results (2-tailed, Yates's  $\chi^2$  test).

### 3.2.4. Subject B-II (family B)

Subject B-II, a sibling of Patient B-I, had a *C9orf72* mutation but did not have symptoms of dementia or motor neuron disease until age 76 (Fig. 1).

## 4. Discussion

We began this study considering patients without family histories of ALS to be SALS because our cohort included only family histories of ALS but not FTD or PPA. Although it may be difficult to describe the real frequency in SALS because 1 of the SALS patients had a family member who developed PPA, the frequencies of the *C9orf72* mutation in Japanese patients were 0.4% (2/552) in SALS and 0% (0/11) in FALS according to this classification. In contrast, the frequencies of the *C9orf72* mutation fall within the ranges of 21%–57% in FALS and 3%–21% in SALS in Western populations (Table 1), and the *C9orf72* mutation has been reported as the most common genetic cause of FALS and SALS in Western populations (Byrne et al.,

2012; Chiò et al., 2012; Cooper-Knock et al., 2012; DeJesus-Hernandez et al., 2011; Gijssels et al., 2012; Majounie et al., 2012; Renton et al., 2011; Sabatelli et al., 2012; Stewart et al., 2012). However, the *C9orf72* mutation in this study was not more frequent than the *SOD1* mutation in Japanese SALS patients (0.4% and 1.6%, Table 1) (Akimoto et al., 2011). Considering these data, the *C9orf72* mutation is more common than the *SOD1* mutation in Western populations but not in Japan, suggesting different genetic backgrounds. Our results may explain the association study of rs2814707 on 9p21.2, which was reported to be the most significantly associated SNP with SALS in Caucasian but not in Japanese and Chinese populations (Iida et al., 2011). A recent report revealed that the rate of expansion in Asian FALS and SALS was 5% (1/20) and 0% (0/238), respectively (Majounie et al., 2012). An analysis of the SNPs on chromosome 9p revealed that all 4 subjects with the *C9orf72* mutation and another Japanese subject from the previously mentioned report (Majounie et al., 2012) share a shorter region of the risk haplotype

than Western populations. Thus, the haplotype bearing the *C9orf72* mutation was only shared in a narrow region between Western and Asian populations, suggesting that the *C9orf72* mutation may be an old mutation in human migration history from Western to East Asia. This mutation was estimated to be approximately 1500 years old (Majounie et al., 2012).

Bulbar onset and cognitive impairment have been reported to be more common in ALS patients with the *C9orf72* repeat expansion (Chiò et al., 2012; Cooper-Knock et al., 2012; DeJesus-Hernandez et al., 2011; Sabatelli et al., 2012; Stewart et al., 2012). We did not find any patients with bulbar onset, but we identified 2 patients with dementia. Although the age at onset has been known to be lower in SALS patients with the *C9orf72* mutation than in those without this mutation (Sabatelli et al., 2012), our patients exhibited a relatively older age at onset (Table 1).

Although apparently sporadic patients with *C9orf72* mutation have been detected worldwide (Byrne et al., 2012; Cooper-Knock et al., 2012; Sabatelli et al., 2012), it was not known whether this phenomenon was due to incomplete penetrance or to spontaneous expansion of the GGGGCC hexanucleotide repeat from a nonpathogenic parental form (ie, a de novo expansion). In this study, we found a 76-year-old healthy individual with a *C9orf72* mutation (Subject B-II), as described in previous studies (Majounie et al., 2012; Renton et al., 2011). This discovery suggests not de novo expansion but incomplete penetrance, which explains the existence of apparently sporadic patients with the *C9orf72* mutation. Although it has been reported that the penetrance of the *C9orf72* mutation is almost full by 80 years by Kaplan–Meier analysis of 603 mutant gene carriers and 5 neurologically healthy individuals, further studies of family members of patients with the *C9orf72* mutation will be required to calculate the true penetrance and to improve genetic counseling.

Finally, we found a PPA patient with the *C9orf72* mutation after detecting the mutation in a SALS patient, suggesting the importance of collecting information regarding whether SALS patients have a family history of dementia or aphasia. Therefore, the possibility of *C9orf72* mutation should be investigated when clinicians meet with SALS patients after determining their family histories of FTD or PPA. Furthermore, our data supported Byrne and colleagues' suggestion that a family history of FTD should also be included in the revised definition of FALS (Byrne et al., 2012).

#### Disclosure statement

All of the authors disclose no conflicts of interest. The study was approved by the ethical committees of the participating centers. All participants gave written informed consent.

#### Acknowledgements

The authors thank all of the participants in this study. The authors also thank Dr. Mariely DeJesus-Hernandez, Dr. Ilse Gijssels, Dr. Marc Cruts, and Dr. Christine Van Broeckhoven for technical advice. This work was supported by the Ministry of Education, Culture, Sports, Science and Technology of Japan (21229011, 21390272, 21591098, 22790817, 22790829, and 23659452), the Ministry of Welfare, Health and Labor of Japan (20261501, 22140501, 22140901, and CCT-B-1701), the Japan Science and Technology Agency, Core Research for Evolutional Science and Technology, and the Inochinoiro Foundation of Japan.

#### Appendix A. Members of the Japanese Consortium for Amyotrophic Lateral Sclerosis Research (JaCALS)

Dr. Mitsuya Morita, Dr. Imaharu Nakano (Division of Neurology, Department of Internal Medicine, Jichi Medical University); Dr. Masashi Aoki (Department of Neurology, Tohoku University School of Medicine); Dr. Koichi Mizoguchi (Department of Neurology, Shizuoka Institute of Epilepsy and Neurological Disorders); Dr. Kazuko Hasegawa (Division of Neurology, National Hospital Organization, Sagami National Hospital); Dr. Akihiro Kawata (Department of Neurology, Tokyo Metropolitan Neurological Hospital); Dr. Ikuko Aiba (Department of Neurology, National Hospital Organization Higashinagoya National Hospital); Dr. Takashi Imai (Division of Neurology, National Hospital Organization, Miyagi National Hospital); Dr. Koichi Okamoto (Department of Neurology, Gunma University Graduate School of Medicine); Dr. Koji Abe (Department of Neurology, Okayama University Graduate School of Medicine); and Dr. Hirohisa Watanabe, Dr. Mizuki Ito, Dr. Jo Senda (Department of Neurology, Nagoya University Graduate School of Medicine).

#### Appendix B. Supplementary data

Supplementary data associated with this article can be found, in the online version, at <http://dx.doi.org/10.1016/j.neurobiolaging.2012.05.011>.

#### References

- Akimoto, C., Morita, M., Atsuta, N., Sobue, G., Nakano, I., 2011. High-Resolution Melting (HRM) Analysis of the Cu/Zn Superoxide Dismutase (SOD1) Gene in Japanese Sporadic Amyotrophic Lateral Sclerosis (SALS) Patients. *Neurol. Res. Int.* 2011, 165415.
- Brooks, B.R., Miller, R.G., Swash, M., Munsat, T.L., 2000. El Escorial revisited: revised criteria for the diagnosis of amyotrophic lateral sclerosis. *Amyotroph. Lateral Scler. Other Mot. Neuron Disord.* 1, 293–299.
- Byrne, S., Elamin, M., Bede, P., Shatunov, A., Walsh, C., Corr, B., Heverin, M., Jordan, N., Kenna, K., Lynch, C., McLaughlin, R.L., Iyer, P.M., O'Brien, C., Phukan, J., Wynne, B., Bokde, A.L., Bradley, D.G., Pender, N., Al-Chalabi, A., Hardiman, O., 2012. Cognitive and clinical characteristics of patients with amyotrophic lateral sclerosis carrying a *C9orf72* repeat expansion: a population-based cohort study. *Lancet Neurol.* 11, 232–240.

- Chiò, A., Borghero, G., Restagno, G., Mora, G., Drepper, C., Traynor, B.J., Sendtner, M., Brunetti, M., Ossola, I., Calvo, A., Pugliatti, M., Sotgiu, M.A., Murru, M.R., Marrosu, M.G., Marrosu, F., Marinou, K., Mandrioli, J., Sola, P., Caponnetto, C., Mancardi, G., Mandich, P., La Bella, V., Spataro, R., Conte, A., Monsunò, M.R., Tedeschi, G., Pisano, F., Bartolomei, I., Salvi, F., Lauria Pinter, G., Simone, I., Logroscino, G., Gambardella, A., Quattrone, A., Lunetta, C., Volanti, P., Zollino, M., Penco, S., Battistini, S., Renton, A.E., Majounie, E., Abramzon, Y., Conforti, F.L., Giannini, F., Corbo, M., Sabatelli, M., ITALSGEN consortium, 2012. Clinical characteristics of patients with familial amyotrophic lateral sclerosis carrying the pathogenic GGGGCC hexanucleotide repeat expansion of C9ORF72. *Brain* 135, 784–793.
- Cooper-Knock, J., Hewitt, C., Highley, J.R., Brockington, A., Milano, A., Man, S., Martindale, J., Hartley, J., Walsh, T., Gelsthorpe, C., Baxter, L., Forster, G., Fox, M., Bury, J., Mok, K., McDermott, C.J., Traynor, B.J., Kirby, J., Wharton, S.B., Ince, P.G., Hardy, J., Shaw, P.J., 2012. Clinico-pathological features in amyotrophic lateral sclerosis with expansions in C9ORF72. *Brain* 135, 751–764.
- DeJesus-Hernandez, M., Mackenzie, I.R., Boeve, B.F., Boxer, A.L., Baker, M., Rutherford, N.J., Nicholson, A.M., Finch, N.A., Flynn, H., Adamson, J., Kouri, N., Wojtas, A., Sengdy, P., Hsiung, G.Y., Karydas, A., Seeley, W.W., Josephs, K.A., Coppola, G., Geschwind, D.H., Wszolek, Z.K., Feldman, H., Knopman, D.S., Petersen, R.C., Miller, B.L., Dickson, D.W., Boylan, K.B., Graff-Radford, N.R., Rademakers, R., 2011. Expanded GGGGCC Hexanucleotide Repeat in Noncoding Region of C9ORF72 Causes Chromosome 9p-Linked FTD and ALS. *Neuron* 72, 245–256.
- Deng, H.X., Chen, W., Hong, S.T., Boycott, K.M., Gorrie, G.H., Siddique, N., Yang, Y., Fecto, F., Shi, Y., Zhai, H., Jiang, H., Hirano, M., Rampersaud, E., Jansen, G.H., Donkervoort, S., Bigio, E.H., Brooks, B.R., Ajroud, K., Sufit, R.L., Haines, J.L., Mugnaini, E., Pericak-Vance, M.A., Siddique, T., 2011. Mutations in UBQLN2 cause dominant X-linked juvenile and adult-onset ALS and ALS/dementia. *Nature* 477, 211–215.
- Gijssels, I., Van Langenhove, T., van der Zee, J., Slegers, K., Philtjens, S., Kleinberger, G., Janssens, J., Bettens, K., Van Cauwenbergh, C., Pereson, S., Engelborghs, S., Sieben, A., De Jonghe, P., Vandenbergh, R., Santens, P., De Bleecker, J., Maes, G., Bäumer, V., Dillen, L., Joris, G., Cuijt, I., Corsmit, E., Elinck, E., Van Dongen, J., Vermeulen, S., Van den Broeck, M., Vaerenberg, C., Mattheijssens, M., Peeters, K., Robberecht, W., Cras, P., Martin, J.J., De Deyn, P.P., Cruts, M., Van Broeckhoven, C., 2012. A C9orf72 promoter repeat expansion in a Flanders-Belgian cohort with disorders of the frontotemporal lobar degeneration-amyotrophic lateral sclerosis spectrum: a gene identification study. *Lancet Neurol.* 11, 54–65.
- Iida, A., Takahashi, A., Deng, M., Zhang, Y., Wang, J., Atsuta, N., Tanaka, F., Kamei, T., Sano, M., Oshima, S., Tokuda, T., Morita, M., Akimoto, C., Nakajima, M., Kubo, M., Kamatani, N., Nakano, I., Sobue, G., Nakamura, Y., Fan, D., Ikegawa, S., 2011. Replication analysis of SNPs on 9p21.2 and 19p13.3 with amyotrophic lateral sclerosis in East Asians. *Neurobiol. Aging* 32, e713–e754.
- International HapMap Consortium, 2003. The International HapMap Project. *Nature* 426, 789–796.
- Laaksovirta, H., Peuralinna, T., Schymick, J.C., Scholz, S.W., Lai, S.L., Myllykangas, L., Sulkava, R., Jansson, L., Hernandez, D.G., Gibbs, J.R., Nalls, M.A., Heckerman, D., Tienari, P.J., Traynor, B.J., 2010. Chromosome 9p21 in amyotrophic lateral sclerosis in Finland: a genome-wide association study. *Lancet Neurol.* 9, 978–985.
- Lomen-Hoerth, C., Anderson, T., Miller, B., 2002. The overlap of amyotrophic lateral sclerosis and frontotemporal dementia. *Neurology* 59, 1077–1079.
- Majounie, E., Renton, A.E., Mok, K., Dopper, E.G., Waite, A., Rollinson, S., Chiò, A., Restagno, G., Nicolaou, N., Simon-Sanchez, J., van Swieten, J.C., Abramzon, Y., Johnson, J.O., Sendtner, M., Pampillet, R., Orrell, R.W., Mead, S., Sidle, K.C., Houlden, H., Rohrer, J.D., Morrison, K.E., Pall, H., Talbot, K., Ansorge, O., Hernandez, D.G., Arepalli, S., Sabatelli, M., Mora, G., Corbo, M., Giannini, F., Calvo, A., Englund, E., Borghero, G., Floris, G.L., Remes, A.M., Laaksovirta, H., McCluskey, L., Trojanowski, J.Q., Van Deerlin, V.M., Schellenberg, G.D., Nalls, M.A., Drory, V.E., Lu, C.S., Yeh, T.H., Ishiura, H., Takahashi, Y., Tsuji, S., Le Ber, I., Brice, A., Drepper, C., Williams, N., Kirby, J., Shaw, P., Hardy, J., Tienari, P.J., Heutink, P., Morris, H.R., Pickering-Brown, S., Traynor, B.J., Chromosome 9-ALS/FTD Consortium; French research network on FTL/FTLD/ALS; ITALSGEN Consortium, 2012. Frequency of the C9orf72 hexanucleotide repeat expansion in patients with amyotrophic lateral sclerosis and frontotemporal dementia: a cross-sectional study. *Lancet Neurol.* 11, 323–330.
- Mok, K., Traynor, B.J., Schymick, J., Tienari, P.J., Laaksovirta, H., Peuralinna, T., Myllykangas, L., Chiò, A., Shatunov, A., Boeve, B.F., Boxer, A.L., DeJesus-Hernandez, M., Mackenzie, I.R., Waite, A., Williams, N., Morris, H.R., Simon-Sanchez, J., van Swieten, J.C., Heutink, P., Restagno, G., Mora, G., Morrison, K.E., Shaw, P.J., Rollinson, P.S., Al-Chalabi, A., Rademakers, R., Pickering-Brown, S., Orrell, R.W., Nalls, M.A., Hardy, J., 2012. The chromosome 9 ALS and FTD locus is probably derived from a single founder. *Neurobiol. Aging* 33, e3–e8.
- Neumann, M., Sampathu, D.M., Kwong, L.K., Truax, A.C., Micsenyi, M.C., Chou, T.T., Bruce, J., Schuck, T., Grossman, M., Clark, C.M., McCluskey, L.F., Miller, B.L., Masliah, E., Mackenzie, I.R., Feldman, H., Feiden, W., Kretschmar, H.A., Trojanowski, J.Q., Lee, V.M., 2006. Ubiquitinated TDP-43 in frontotemporal lobar degeneration and amyotrophic lateral sclerosis. *Science* 314, 130–133.
- Renton, A.E., Majounie, E., Waite, A., Simón-Sánchez, J., Rollinson, S., Gibbs, J.R., Schymick, J.C., Laaksovirta, H., van Swieten, J.C., Myllykangas, L., Kalimo, H., Paetau, A., Abramzon, Y., Remes, A.M., Kaganovich, A., Scholz, S.W., Duckworth, J., Ding, J., Harmer, D.W., Hernandez, D.G., Johnson, J.O., Mok, K., Ryten, M., Trabzuni, D., Guerreiro, R.J., Orrell, R.W., Neal, J., Murray, A., Pearson, J., Jansen, I.E., Sondervan, D., Seelaar, H., Blake, D., Young, K., Halliwell, N., Callister, J.B., Toulson, G., Richardson, A., Gerhard, A., Snowden, J., Mann, D., Neary, D., Nalls, M.A., Peuralinna, T., Jansson, L., Isoviiita, V.M., Kaivorinne, A.L., Holtta-Vuori, M., Ikonen, E., Sulkava, R., Benatar, M., Wu, J., Chiò, A., Restagno, G., Borghero, G., Sabatelli, M., Heckerman, D., Rogaeva, E., Zinman, L., Rothstein, J.D., Sendtner, M., Drepper, C., Eichler, E.E., Alkan, C., Abdullaev, Z., Pak, S.D., Dutra, A., Pak, E., Hardy, J., Singleton, A., Williams, N.M., Heutink, P., Pickering-Brown, S., Morris, H.R., Tienari, P.J., Traynor, B.J., ITALSGEN Consortium, 2011. A Hexanucleotide Repeat Expansion in C9ORF72 Is the Cause of Chromosome 9p21-Linked ALS-FTD. *Neuron* 72, 257–268.
- Sabatelli, M., Conforti, F.L., Zollino, M., Mora, G., Monsunò, M.R., Volanti, P., Marinou, K., Salvi, F., Corbo, M., Giannini, F., Battistini, S., Penco, S., Lunetta, C., Quattrone, A., Gambardella, A., Logroscino, G., Simone, I., Bartolomei, I., Pisano, F., Tedeschi, G., Conte, A., Spataro, R., La Bella, V., Caponnetto, C., Mancardi, G., Mandich, P., Sola, P., Mandrioli, J., Renton, A.E., Majounie, E., Abramzon, Y., Marrosu, F., Marrosu, M.G., Murru, M.R., Sotgiu, M.A., Pugliatti, M., Rodolico, C., ITALSGEN Consortium, Moglia, C., Calvo, A., Ossola, I., Brunetti, M., Traynor, B.J., Borghero, G., Restagno, G., Chiò, A., 2012. C9ORF72 hexanucleotide repeat expansions in the Italian sporadic ALS population. *Neurobiol. Aging* 33, e15–e20.
- Stewart, H., Rutherford, N.J., Briemberg, H., Krieger, C., Cashman, N., Fabros, M., Baker, M., Fok, A., DeJesus-Hernandez, M., Eisen, A., Rademakers, R., Mackenzie, I.R., 2012. Clinical and pathological features of amyotrophic lateral sclerosis caused by mutation in the C9ORF72 gene on chromosome 9p. *Acta Neuropathol.* 123, 409–417.
- Ticozzi, N., Tiloca, C., Morelli, C., Colombrita, C., Poletti, B., Doretti, A., Maderia, L., Messina, S., Ratti, A., Silani, V., 2011. Genetics of familial Amyotrophic lateral sclerosis. *Arch. Ital. Biol.* 149, 65–82.
- Valdman, P.N., Daoud, H., Dion, P.A., Rouleau, G.A., 2009. Recent advances in the genetics of amyotrophic lateral sclerosis. *Curr. Neurol. Neurosci. Rep.* 9, 198–205.